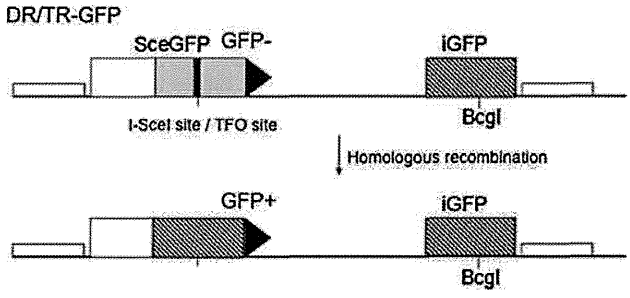

Fig. 2 DR-GFP assay. In the *DR-GFP* substrate, an I-SceI site is inserted into the GFP gene on sceGFP. GFP is inactivated by the stop-codon in the I-SceI site. To restore functionality of the *GFP* gene, the *iGFP* gene has .8 kb of sequence homology to direct the repair of an I-*Sce*I-cleaved *SceGFP* gene

have demonstrated the involvement of the FA pathway overall, may facilitate delineation of the mechanisms and factors involved in this process.

Diamond–Blackfan anemia

Diamond–Blackfan anemia (DBA) is a rare congenital bone marrow failure syndrome characterized by severe normochromic macrocytic anemia and reticulocytopenia, with selective hypoplasia of erythroid precursors in the bone marrow. Up to 50 % of affected individuals have physical abnormalities including short stature, craniofacial dysmorphism, heart defects, and anomalies of the thumbs and genitourinary tract [20]. Increased risk of malignant disease, such as acute myeloid leukemia and osteogenic sarcoma, has also been reported to occur in this syndrome [21]. The incidence of DBA has been estimated to be 5–7 per million live births in Europe and North America. In a national study conducted in Japan between 2006 and 2010, 65 new DBA patients were registered. During this study period, the mean number of live births per year in Japan was reported to be 1.08 million, putting the incidence of DBA at 12 per each million live births, as most of these patients were diagnosed as DBA during infancy. The majority of these patients are sporadic, with the percentages of patients with autosomal dominant inheritance reported to be less than 10 %. Corticosteroids are recommended as a first line therapy, as these have been reported to improve erythropoiesis in approximately 80 % of DBA patients. In patients refractory to corticosteroids or who develop other forms of cytopenia, HSC transplantation has been suggested as a viable alternative [22].

Molecular pathogenesis

The first DBA gene (RPS19) was identified in 1999 and was found in approximately 25 % of the probands in western countries [23]. Since then, a total of nine genes encoding large (RPL) or small (RPS) ribosomal subunit proteins were found to be mutated in DBA patients, including RPL5 (6.6 %), RPL11 (4.8 %), RPL35A (3 %), RPS24 (2 %), RPS17 (1 %), RPS7 (1 %), RPS10 (6.4 %), and RPS26 (2.6 %) [24] (Table 2). Collectively, mutations in at least one of these nine genes have been detected in approximately 50–60 % of DBA patients. Of 68 Japanese been examined, mutations in RPS 19, RPL5, RPL11, RPS17, RPS26 were identified in 10 (14.7 %), six (8.8 %), three (4.4 %), one (1.5 %), one (1.5 %), and one (1.5 %), respectively. These mutations have subsequently been determined to occur in 32.4 % of Japanese patients [25, 26]. A low incidence of mutations in the RPS19 gene may account for the overall lower incidence of total mutations in the Japanese population.

As conventional gene sequencing cannot identify large gene deletions, there have been only a few reports of patients with allelic losses in the RPS19 and RPL35A genes. Kuramitsu et al. [26] investigated large deletions of the RP genes using gene copy number variation analysis based on a quantitative-PCR and a single-nucleotide polymorphism (SNP) array. This study used sequencing to screen for large gene deletion in 27 patients without gene mutations. The PCR-based gene copy number assay identified a large deletion in seven (25.9 %) of 27 patients. Of these, three patients had RPS17, two had RPS19, one had RPL5, while one had RPL35A deletions. The SNP array confirmed six of the seven large deletions. Based on these new methods, the frequency of RP gene abnormalities in the DBA patients increased to 42.6 %. All patients with large deletions in DBA genes exhibited malformation with growth retardation. However, half of the patients with a mutation due to sequencing had growth retardation, while all seven patients with a large deletion exhibited growth retardation. While four of seven patients responded to corticosteroids, there were no phenotypic

Table 2 Ribosomal protein gene mutations and deletions in 68 Japanese patients with Diamond–Blackfan anemia

Gene	Mutation	Deletion	Total (%)
RPS 19	10	2	12 (17.6 %)
RPL 5	6	1	7 (10.3 %)
RPS 17	3	0	3 (4.4 %)
RPL 11	3	1	4 (5.9 %)
RPS 10	1	0	1 (1.5 %)
RPS 26	1	0	1 (1.5 %)
RPS 35A	0	1	1 (1.5 %)
RPS 24	0	0	0
RPS 14	0	0	0
Total	22	7	29 (42.6 %)

differences noted between patients with and without large deletions, including response rate to corticosteroids and other malformations.

Farrar et al. [27] also identified RP gene deletions in nine (17 %) of 51 patients without any identifiable mutation by SNP array. Of these nine patients, three had RPS17, two had RPS26, two had RPS19, and two had RPL35A deletions. Clinically, five of the nine patients responded to corticosteroids. Two exhibited short stature. These two studies suggested that genomic deletions may be detected in 4–10 % of DBA patients, which is more common than has been previously suspected. Thus, in addition to conventional gene sequencing, molecular studies of suspected DBA cases should also include either a SNP array or PCR-based gene copy number assay.

Despite extensive sequencing of all the RP genes, at present mutations have only been found in approximately half of DBA patients examined, which raises the question whether other genes are responsible for DBA. Recent advance in genomic sequencing have made it possible to search for new candidate genes. Sankaran et al. [28] performed exome sequencing on two siblings without RP gene mutations. Both affected siblings satisfied the diagnostic criteria for DBA and both parents had normal blood values, suggesting X-linked or autosomal recessive inheritance. During sequencing, at least 10-fold coverage was obtained in more than 93 % of the target bases. After filtering, a total of 74 variants were identified as being shared by the three affected siblings. Of these 74 mutations, 31 were found in two affected siblings but not in the unaffected sibling. No variants were identified that would fit an autosomal recessive model of inheritance. Only the GATA1 gene showed appropriate segregation for an X-linked disease with full penetrance. The mutation in the GATA1 gene is a G-C transversion at position 48,649,736 on the X chromosome and results in a substitution of leucine for valine at amino acid 74 of the GATA1 protein. This mutation impaired production of the full-length form of the exon 2 protein. After screening 62 additional male DBA patients without known mutations for the GATA1 mutation, the study also identified one patient with a mutation in GATA1 at the exon 2-intron 2 junction. It was predicted that this would result in impaired splicing and a frameshift of the full-length GATA1 open reading frame. Overall, this study has opened new avenues for studying the molecular pathogenesis of DBA.

Role of p53 in the pathophysiology of DBA

Although current evidence suggests that impaired ribosomal biogenesis should affect all blood cell lineages, one question remains as to why it affects only the erythroid progenitors. Several animal models have demonstrated the role of p53 in the pathophysiology of DBA. The RPS19-deficient zebrafish model has been shown to have many features of DBA and is accompanied by the up-regulation of the p53 family [29]. Suppression of p53 in the RPS19-deficient zebrafish alleviated the phenotype and improved survival. RPS19 knockdown mouse fetal liver cells, which were created by retrovirus-infected siRNA, showed reduced proliferation but normal differentiation of erythroid cells and an increased level of p53 and p21 [30]. Dutt et al. [31] have examined the accumulation and activity of p53 in different hematopoietic lineages after a partial knockdown of the RPS19 gene in primary human bone marrow-derived CD34 cells. Their study showed that p53 accumulates selectively in erythroid progenitors, resulting in lineage-specific p53 target gene expression, cell cycle arrest, and apoptosis. While pifithrin-α has been shown to inhibit the activity of p53, nutlin-3 activates p53 through the inhibition of HDM2. In addition, nutlin-3 selectivity impairs erythropoiesis, whereas inhibition of p53 by pifithrin-α rescues the erythroid defect. To directly examine whether p53 accumulation is operative in patients with DBA, bone marrow biopsies from eight patients with DBA were stained with anti-human p53 antibody and shown to have strong nuclear staining in two patients and weak nuclear staining in six patients. The erythroid lineage has a low threshold for the induction of p53, which accounts for the selective impaired erythropoiesis in patients with DBA.

Alternative therapies for DBA

Although approximately 80 % of DBA patients initially respond to corticosteroid, half of the responders are steroid-dependent. Only 20 % of these patients achieve remission. Although historically many alternative drugs have been tried, there has been no agreement on a second-line therapy. L-leucine is an essential amino acid and is known to be an activator of mRNA and stimulate protein synthesis through the mammalian target of rapamycin (mTOR) pathway. L-leucine treatment of the RPS19-deficient zebrafish model results in a striking improvement of anemia and developmental defects. These findings were reproduced in primary human CD34 cells after knockdown of the RPS19 gene [32]. Therapeutic effect of L-leucine has also been confirmed in the mouse model for RPS19-deficient DBA and shown to be associated with reduced p53 activity in hematopoietic progenitors [33]. Recently, leucine has been used on an investigational basis in one patient with DBA and is reported to have achieved a remission [34].

These findings support commencement of a clinical trial with L-leucine as an alternative therapy for DBA.

Dyskeratosis congenita

Clinical features of patients with dyskeratosis congenita

Dyskeratosis congenita (DC) is a rare inherited disease characterized by the classical mucocutaneous triad of abnormal skin pigmentation, nail dystrophy, and mucosal leucoplakia in approximately 80–90 % of patients [34]. Patients with DC are unable to maintain the telomere complex that protects the chromosome ends and consequently have very short telomeres [35]. Shortened telomeres can cause a wide variety of clinical features across a phenotypic spectrum consisting not only of mucocutaneous abnormalities but also multisystem symptoms including bone marrow failure, pulmonary fibrosis, hepatic fibrosis, and predisposition to malignancy [36, 37]. Indeed, non-mucocutaneous features, such as bone marrow failure and pulmonary fibrosis, occasionally precede mucocutaneous abnormalities, making it difficult to diagnose patients with DC based on clinical features alone. The incidence of DC is estimated to be one per million live births.

The diagnostic criteria for DC proposed by Vulliamy [38] include one or more of the three classic mucocutaneous features combined with hypoplastic bone marrow and at least two other somatic features known to occur in DC. The primary causes of mortality in patients with DC are bone marrow failure syndrome (60–70 %), pulmonary complications (10–15 %), and malignancy (particularly MDS and AML) (10 %) [36, 37].

Genetic background of DC

DC is a genetically heterogeneous disorder, showing autosomal recessive, autosomal dominant, and X-linked inheritance. The *DKC1* gene on chromosome (chr) Xq28, which encodes dyskerin, was the first gene identified in the X-linked DC patients [39]. Dyskerin has a close association with the RNA component of telomerase (*TERC*), and mutations in dyskerin cause a reduction in accumulation of *TERC* and reduced telomere length [35]. In addition to its role in the biogenesis of telomerase RNA dyskerin is involved in ribosomal RNA biogenesis. Dyskerin catalyzes uridine to pseudouridine, which is a critical step for ribosomal RNA maturation and function. These findings imply that both telomere and ribosomal defects may occur in patients with *DKC1* mutations. Subsequently, heterozygous *TERC* mutations have also been found in autosomal dominant DC patients [40]. Genetic screening has identified mutations of other components of the telomerase complex, including *TERT* (chr 5p15) [41, 42], *NOP10* (chr 15q14-q15) [43], and *NHP2* (chr 5q35) [44] in patients with rare autosomal recessive DC. Mutations of *TERT* have also been reported in the autosomal dominant family [45]. Moreover, heterozygous mutations of *TINF2* (chr 14q12) that encode TIN2, which is the main component of shelterin and which protects telomeres, have been identified in <11 % of DC patients [46, 47].

More recently, mutations of *TCAB1* (chr 17p13) were identified in patients with DC as autosomal recessive forms [48]. Venteicher et al. [49] found that TCAB1 associates with TERT, dyskerin and TERC, and small Cajal body RNAs (scaRNAs) that are involved in modifying splicing RNAs to control telomerase trafficking. TCAB1 defects prevented TERC from associating with the Cajal bodies, which disrupted the telomerase–telomere association. A recent case report described biallelic mutations of the *CTC1* gene (chr 17p13) in a patient with DC [50]. This gene was originally described as causative gene of the Coats plus syndrome, which is a form of cerebroretinal microangiopathy with calcifications and cysts (CRMCC). The mutation frequencies of these new genes for DC remain unknown.

At present, eight of the mutated genes in DC have been shown to be associated with the telomerase holoenzyme (TERT, *TERC, DKC1, NOP10, NHP2, TCAB1,* and *CTC1)* or the shelterin complex (TINF2), accounting for approximately 50 % of DC patients. Mutations in telomerase and telomere components have also been identified in patients with aplastic anemia, pulmonary fibrosis, and liver diseases that did not have any mucocutaneous manifestations [45, 46, 51–59]. These findings suggest that defective telomere maintenance causes not only classical DC, but also a broad spectrum of diseases previously thought to be idiopathic and thus this has led to a new concept of diseases termed ''syndromes of telomere shortening''.

Cryptic DC patients in aplastic anemia

Patients with DC have been shown to have disease diversity in terms of age at onset, symptoms, and severity. This diversity occurs even among the patients with the same gene mutation. Bone marrow failure sometimes precedes mucocutaneous manifestations in patients with DC, and a substantial proportion of patients with aplastic anemia have shorter telomeres compared with normal individuals [60, 61]. These observations have prompted screening for gene mutations responsible for telomere maintenance in patients with aplastic anemia and other bone marrow failure syndromes. This screening identified mutations in *TERC* and *TERT* in 3 % of the aplastic anemia patients [54, 55]. Our research group conducted a study in Japanese children with aplastic anemia and identified two of 96 as having the *TERT* mutations, although none of the patients had a *TERC* mutation [53]. Patients with *TERC* or *TERT* mutations have been shown to have very short telomeres in their blood cells. Recently, Du et al. [52] found that 6 (5.5 %) of 109

pediatric patients with severe aplastic anemia had mutations of *TINF2*. In an unpublished study, our research group screened for mutations of *TINF2* and found that of the 96 pediatric patients with aplastic anemia that were examined, none exhibited any mutations of this gene.

Three methods are commonly used for measuring telomere length, including Southern blot, real-time polymerase chain reaction, and flow cytometry and fluorescence in situ hybridization (flow-FISH). Of these, the flow-FISH has been shown to be the most appropriate when undertaking ''prospective'' screening [62, 63]. As shown in Fig. 3, patients with DC and aplastic anemia with the *TERT* mutation were all found to have very short telomeres as compared with the idiopathic aplastic anemia patients and normal individuals. As a small subset of patients with apparently idiopathic aplastic anemia have been shown to carry telomere gene mutations, identification of such patients is critical for informing treatment decisions. Aplastic anemia patients should be routinely screened for telomere gene mutations prior to starting any treatment. However, because screening of gene mutations can be both laborious and time consuming, we have adopted the screening of telomere length in blood cells rather than screening of gene mutations.

It should be noted that short telomeres are not specific for patients with DC, as they are also seen in patients with other bone marrow failure syndromes. Although short telomeres have also been found in patients with other congenital bone marrow failure syndromes, such as Shwachman–Diamond syndrome and Fanconi anemia, telomere lengths in patients with DC have been demonstrated to be shorter than those in all other bone marrow failure syndromes. In fact, telomere length in most patients with DC is below the first percentile of telomere length found in healthy controls [64].

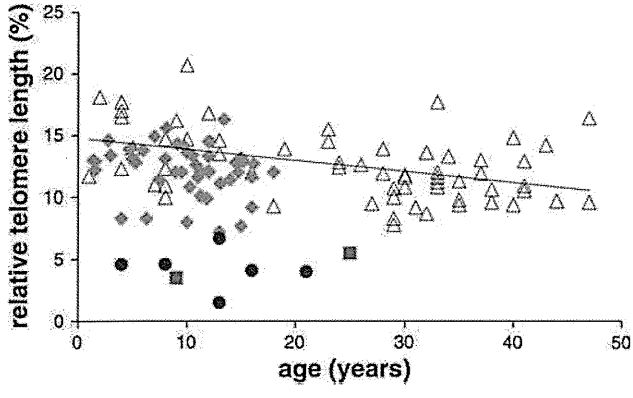

Fig. 3 Relative telomere length in peripheral blood lymphocytes from patients with dyskeratosis congenita (*filled circles*), patients with aplastic anemia harboring TERT mutations (*filled squares*), patients with idiopathic aplastic anemia (*filled argyles*) and normal individuals (*open triangles*). Telomere lengths were measured by flow cytometry-fluorescent in situ hybridization (flow-FISH). Relative telomere length was calculated as the ratio between the telomere signal of each sample and the telomere signal of the control cell line (cell line 1301). These data were provided by the Department of Pediatrics, Nagoya University Graduate School of Medicine

Family members of patients with DC should receive genetic counseling to rule out if they are silent carriers. In particular, genetic counseling is necessary during the proband search for a donor for HSC transplantation. Studies on telomere length analyses in families with DC have shown that mutated carriers with clinical signs of bone marrow failure have short telomeres. Even so, telomere length cannot predict the presence or absence of a mutation in family members with bone marrow failure. In addition, there have been rare cases that show normal telomere length, even though the subject harbors the same mutation as the proband. This suggests that mutation alone does not sufficiently explain the reduction of telomere length [51].

Clinical management for DC

Bone marrow failure and immune deficiency are the most common causes of death in up to 60–70 % of patients with DC. Androgen (e.g. oxymetholone) has been used to improve cytopenia in patients with DC since the 1960s. However, the mechanism of action of androgen has not been well understood until recently. Calado et al. [65] showed that in vitro exposure of normal peripheral blood cells to androgen produced higher TERT mRNA levels. When these patients were treated with cells from patients who had a heterozygous mutation of the telomerase, it was possible to restore their low baseline telomerase activity to normal levels. Thus, as telomere shortening is closely associated with malignant disease, androgen therapy might be able to prevent or postpone the development of various types of cancers. Erythropoietin and/or G-CSF combined with androgen has occasionally provided transient hematopoietic recovery to poor responders to androgen alone [66]. However, this combination should be used with caution, as severe splenic peliosis and fatal rupture have been reported in two patients with DC who received simultaneous administration of androgen and G-CSF [67].

Allogeneic HSC transplantation is the only curative treatment for bone marrow failure in patients with DC. However, the outcome in previous reports has been disappointing due to unacceptable transplant-related toxicities, including severe pulmonary/liver complications, especially in transplants from an alternative donor [68, 69]. To avoid these complications, non-myeloablative conditioning regimens have been recently used in several cases. Dietz et al. [70] reported encouraging results of six patients with DC who received a fludarabine-based non-myeloablative regimen. Of the four surviving patients, three were recipients of unrelated grafts. Non-myeloablative

transplants are expected to provide improvement in the short-term survival. At our institute, three patients with DC underwent allogeneic bone marrow transplantation following non-myeloablative conditioning from 2003 to 2009. Successful engraftment was achieved in all patients with only a few regimen-related toxicities, and at the present time all continue to survive without any symptoms [71]. However, due the late effects of conditioning agents and allogeneic immune responses within the recipient's organs, such as the lung and liver, longer-term follow-ups are necessary to definitively clarify the present results.

Conclusion

Although recent studies have identified many causative genes, mutations of these genes have only been found in half of the patients with DBA or DKC. Next-generation sequencing (or massive parallel sequencing) technologies have led to a tremendous revolution in genomics, with their effects currently becoming increasingly widespread. This new strategy may soon be able to reveal the remaining unknown causative genes in IBMFS.

Recently, Agarwal et al. [72] established induced pluripotent stem cells (iPSCs) derived from a patient with DC and showed that the reprogrammed DC cells overcame a critical limitation in TERC levels to restore the telomere maintenance and self-renewal. These findings indicate that drugs or gene therapy that upregulate TERC activity may show therapeutic potential in patients with DC. These same strategies may also be applicable for other IBMFS.

The only long-term curative treatment for bone marrow failure in patients with IBMFS is allogeneic HSC transplantation, although this procedure has a risk of severe adverse effects. Multicenter prospective studies are needed to establish appropriate conditioning regimens aimed at reducing transplant-related mortality. Future studies must aim to improve short-term outcomes, such as hematological recovery, and to decrease the incidence of late adverse effects.

References

1. Joenje H, Patel KJ. The emerging genetic and molecular basis of Fanconi anaemia. Nat Rev Genet. 2001;2:446–57.
2. Kim H, D'Andrea AD. Regulation of DNA cross-link repair by the Fanconi anemia/BRCA pathway. Genes Dev. 2012;26: 1393–408.
3. D'Andrea AD, Grompe M. The Fanconi anaemia/BRCA pathway. Nat Rev Cancer. 2003;3:23–34.
4. Alter BP, Rosenberg PS, Brody LC. Clinical and molecular features associated with biallelic mutations in FANCD1/BRCA2. J Med Genet. 2007;44:1–9.
5. Rosenberg PS, Socie G, Alter BP, Gluckman E. Risk of head and neck squamous cell cancer and death in patients with Fanconi anemia who did and did not receive transplants. Blood. 2005; 105:67–73.
6. Whitney MA, Saito H, Jakobs PM, Gibson RA, Moses RE, Grompe M. A common mutation in the FACC gene causes Fanconi anaemia in Ashkenazi Jews. Nat Genet. 1993;4:202–5.
7. Gibson RA, Hajianpour A, Murer-Orlando M, Buchwald M, Mathew CG. A nonsense mutation and exon skipping in the Fanconi anaemia group C gene. Hum Mol Genet. 1993;2:797–9.
8. Garcia-Higuera I, Taniguchi T, Ganesan S, Meyn MS, Timmers C, Hejna J, et al. Interaction of the Fanconi anemia proteins and BRCA1 in a common pathway. Mol Cell. 2001;7:249–62.
9. Smogorzewska A, Matsuoka S, Vinciguerra P, McDonald ER 3rd, Hurov KE, Luo J, et al. Identification of the FANCI protein, a monoubiquitinated FANCD2 paralog required for DNA repair. Cell. 2007;129:289–301.
10. Carreau M. Not-so-novel phenotypes in the Fanconi anemia group D2 mouse model. Blood. 2004;103:2430.
11. Marietta C, Thompson LH, Lamerdin JE, Brooks PJ. Acetaldehyde stimulates FANCD2 monoubiquitination, H2AX phosphorylation, and BRCA1 phosphorylation in human cells in vitro: implications for alcohol-related carcinogenesis. Mutat Res. 2009;664:77–83.
12. Langevin F, Crossan GP, Rosado IV, Arends MJ, Patel KJ. Fancd2 counteracts the toxic effects of naturally produced aldehydes in mice. Nature. 2011;475:53–8.
13. Garaycoechea JI, Crossan GP, Langevin F, Daly M, Arends MJ, Patel KJ. Genotoxic consequences of endogenous aldehydes on mouse haematopoietic stem cell function. Nature. 2012;489: 571–5.
14. Moynahan ME, Chiu JW, Koller BH, Jasin M. Brca1 controls homology-directed DNA repair. Mol Cell. 1999;4:511–8.
15. Moynahan ME, Pierce AJ, Jasin M. BRCA2 is required for homology-directed repair of chromosomal breaks. Mol Cell. 2001;7:263–72.
16. Nakanishi K, Yang YG, Pierce AJ, Taniguchi T, Digweed M, D'Andrea AD, et al. Human Fanconi anemia monoubiquitination pathway promotes homologous DNA repair. Proc Natl Acad Sci USA. 2005;102:1110–5.
17. Raschle M, Knipscheer P, Enoiu M, Angelov T, Sun J, Griffith JD, et al. Mechanism of replication-coupled DNA interstrand crosslink repair. Cell. 2008;134:969–80.
18. Knipscheer P, Raschle M, Smogorzewska A, Enoiu M, Ho TV, Scharer OD, et al. The Fanconi anemia pathway promotes replication-dependent DNA interstrand cross-link repair. Science. 2009;2009(326):1698–701.
19. Nakanishi K, Cavallo F, Perrouault L, Giovannangeli C, Moynahan ME, Barchi M, et al. Homology-directed Fanconi anemia pathway cross-link repair is dependent on DNA replication. Nat Struct Mol Biol. 2011;18:500–3.
20. Alter BP, Young NS. The bone marrow failure syndromes. In: Nathan DG, Orkin HS, editors. Hematology of infancy and childhood, vol 1. Philadelphia: Saunders; 1998. p. 237–335.
21. Vlachos A, Rosenberg PS, Atsidaftos E, Alter BP, Lipton JM. Incidence of neoplasia in Diamond Blackfan anemia: a report from the Diamond Blackfan Anemia Registry. Blood. 2012;119: 3815–9.
22. Mugishima H, Ohga S, Ohara A, Kojima S, Fujisawa K, For the Aplastic Anemia Committee of the Japanese Society of Pediatric Hematology. Hematopoietic stem cell transplantation for Diamond–Blackfan anemia: a report from the Aplastic Anemia Committee of the Japanese Society of Pediatric Hematology. Pediatr Transpl. 2007;11:601–7.
23. Draptchinskaia N, Gustavsson P, Andersson B, Pettersson M, Willig TN, Dianzani I, et al. The gene encoding ribosomal

protein S19 is mutated in Diamond–Blackfan anaemia. Nat Genet. 1999;21:169–75.
24. Boria I, Garelli E, Gazda HT, Aspesi A, Quarello P, Pavesi E, et al. The ribosomal basis of Diamond–Blackfan anemia: mutation and database update. Hum Mutat. 2010;31:1269–79.
25. Konno Y, Toki T, Tandai S, Xu G, Wang R, Terui K, et al. Mutations in the ribosomal protein genes in Japanese patients with Diamond–Blackfan anemia. Haematologica. 2010;95: 1293–9.
26. Kuramitsu M, Sato-Otsubo A, Morio T, Takagi M, Toki T, Terui K, et al. Extensive gene deletions in Japanese patients with Diamond–Blackfan anemia. Blood. 2012;119:2376–84.
27. Farrar JE, Vlachos A, Atsidaftos E, Carlson-Donohoe H, Markello TC, Arceci RJ, et al. Ribosomal protein gene deletions in Diamond–Blackfan anemia. Blood. 2011;118:6943–51.
28. Sankaran VG, Ghazvinian R, Do R, Thiru P, Vergilio JA, Beggs AH, et al. Exome sequencing identifies GATA1 mutations resulting in Diamond–Blackfan anemia. J Clin Invest. 2012;122: 2439–43.
29. Danilova N, Sakamoto KM, Lin S. Ribosomal protein S19 deficiency in zebrafish leads to developmental abnormalities and defective erythropoiesis through activation of p53 protein family. Blood. 2008;112:5228–37.
30. Sieff CA, Yang J, Merida-Long LB, Lodish HF. Pathogenesis of the erythroid failure in Diamond Blackfan anaemia. Br J Haematol. 2010;148:611–22.
31. Dutt S, Narla A, Lin K, Mullally A, Abayasekara N, Megerdichian C, et al. Haploinsufficiency for ribosomal protein genes causes selective activation of p53 in human erythroid progenitor cells. Blood. 2011;117:2567–76.
32. Payne EM, Virgilio M, Narla A, Sun H, Levine M, Paw BH, et al. L-leucine improves the anemia and developmental defects associated with Diamond–Blackfan anemia and del(5q) MDS by activating the mTOR pathway. Blood. 2012;120:2214–24.
33. Jaako P, Debnath S, Olsson K, Bryder D, Flygare J, Karlsson S. Dietary L-leucine improves the anemia in a mouse model for Diamond–Blackfan anemia. Blood. 2012;120:2225–8.
34. Kirwan M, Dokal I. Dyskeratosis congenita, stem cells and telomeres. Biochim Biophys Acta. 2009;1792:371–9.
35. Mitchell JR, Wood E, Collins K. A telomerase component is defective in the human disease dyskeratosis congenita. Nature. 1999;402:551–5.
36. Dokal I. Dyskeratosis congenita in all its forms. Br J Haematol. 2000;110:768–79.
37. Walne AJ, Dokal I. Advances in the understanding of dyskeratosis congenita. Br J Haematol. 2009;145:164–72.
38. Vulliamy TJ, Marrone A, Knight SW, Walne A, Mason PJ, Dokal I. Mutations in dyskeratosis congenita: their impact on telomere length and the diversity of clinical presentation. Blood. 2006;107: 2680–5.
39. Heiss NS, Knight SW, Vulliamy TJ, Klauck SM, Wiemann S, Mason PJ, Poustka A, Dokal I. X-linked dyskeratosis congenita is caused by mutations in a highly conserved gene with putative nucleolar functions. Nat Genet. 1998;19:32–8.
40. Vulliamy T, Marrone A, Goldman F, Dearlove A, Bessler M, Mason PJ, et al. The RNA component of telomerase is mutated in autosomal dominant dyskeratosis congenita. Nature. 2001;413: 432–5.
41. Armanios M, Chen JL, Chang YP, Brodsky RA, Hawkins A, Griffin CA, et al. Haploinsufficiency of telomerase reverse transcriptase leads to anticipation in autosomal dominant dyskeratosis congenita. Proc Natl Acad Sci USA. 2005;102:15960–4.
42. Marrone A, Walne A, Tamary H, Masunari Y, Kirwan M, Beswick R, et al. Telomerase reverse-transcriptase homozygous mutations in autosomal recessive dyskeratosis congenita and Hoyeraal–Hreidarsson syndrome. Blood. 2007;110:4198–205.
43. Walne AJ, Vulliamy T, Marrone A, Beswick R, Kirwan M, Masunari Y, et al. Genetic heterogeneity in autosomal recessive dyskeratosis congenita with one subtype due to mutations in the telomerase-associated protein NOP10. Hum Mol Genet. 2007;16: 1619–29.
44. Vulliamy T, Beswick R, Kirwan M, Marrone A, Digweed M, Walne A, et al. Mutations in the telomerase component NHP2 cause the premature ageing syndrome dyskeratosis congenita. Proc Natl Acad Sci USA. 2008;105:8073–8.
45. Vulliamy TJ, Walne A, Baskaradas A, Mason PJ, Marrone A, Dokal I. Mutations in the reverse transcriptase component of telomerase (TERT) in patients with bone marrow failure. Blood Cells Mol Dis. 2005;34:257–63.
46. Walne AJ, Dokal I. Dyskeratosis congenita: a historical perspective. Mech Ageing Dev. 2008;129:48–59.
47. Savage SA, Giri N, Baerlocher GM, Orr N, Lansdorp PM, Alter BP. TINF2, a component of the shelterin telomere protection complex, is mutated in dyskeratosis congenita. Am J Hum Genet. 2008;82:501–9.
48. Zhong F, Savage SA, Shkreli M, et al. Disruption of telomerase trafficking by TCAB1 mutation causes dyskeratosis congenita. Genes Dev. 2011;25:11–6.
49. Venteicher AS, Abreu EB, Meng Z, McCann KE, Terns RM, Veenstra TD, Terns MP, Artandi SE. A human telomerase holoenzyme protein required for Cajal body localization and telomere synthesis. Science. 2009;323:644–8.
50. Keller RB, Gagne KE, Usmani GN, Asdourian GK, Williams DA, Hofmann I, Agarwal S. CTC1 Mutations in a patient with dyskeratosis congenita. Pediatr Blood Cancer. 2012;59:311–4.
51. Du HY, Pumbo E, Ivanovich J, An P, Maziarz RT, Reiss UM, et al. TERC and TERT gene mutations in patients with bone marrow failure and the significance of telomere length measurements. Blood. 2009;113:309–16.
52. Du HY, Mason PJ, Bessler M, Wilson DB. TINF2 mutations in children with severe aplastic anemia. Pediatr Blood Cancer. 2009;52:687.
53. Liang J, Yagasaki H, Kamachi Y, Hama A, Matsumoto K, Kato K, et al. Mutations in telomerase catalytic protein in Japanese children with aplastic anemia. Haematologica. 2006;91:656–8.
54. Yamaguchi H, Calado RT, Ly H, Kajigaya S, Baerlocher GM, Chanock SJ, et al. Mutations in TERT, the gene for telomerase reverse transcriptase, in aplastic anemia. N Engl J Med. 2005; 352:1413–24.
55. Yamaguchi H, Baerlocher GM, Lansdorp PM, Chanock SJ, Nunez O, Sloand E, et al. Mutations of the human telomerase RNA gene (TERC) in aplastic anemia and myelodysplastic syndrome. Blood. 2003;102:916–8.
56. Vulliamy T, Marrone A, Dokal I, Mason PJ. Association between aplastic anaemia and mutations in telomerase RNA. Lancet. 2002;359:2168–70.
57. Tsakiri KD, Cronkhite JT, Kuan PJ, Xing C, Raghu G, Weissler JC, et al. Adult-onset pulmonary fibrosis caused by mutations in telomerase. Proc Natl Acad Sci USA. 2007;104:7552–7.
58. Armanios MY, Chen JJ, Cogan JD, Alder JK, Ingersoll RG, Markin C, et al. Telomerase mutations in families with idiopathic pulmonary fibrosis. N Engl J Med. 2007;356:1317–26.
59. Calado RT, Regal JA, Kleiner DE, Schrump DS, Peterson NR, Pons V, et al. A spectrum of severe familial liver disorders associate with telomerase mutations. PLoS ONE. 2009;4:e 7926.
60. Ball SE, Gibson FM, Rizzo S, Tooze JA, Marsh JC, Gordon-Smith EC. Progressive telomere shortening in aplastic anemia. Blood. 1998;91:3582–92.
61. Lee JJ, Kook H, Chung IJ, Na JA, Park MR, Hwang TJ, et al. Telomere length changes in patients with aplastic anaemia. Br J Haematol. 2001;112:1025–30.

62. Baerlocher GM, Vulto I, de Jong G, Lansdorp PM. Flow cytometry and FISH to measure the average length of telomeres (flow FISH). Nat Protoc. 2006;1:2365–76.
63. Canela A, Klatt P, Blasco MA. Telomere length analysis. Methods Mol Biol. 2007;371:45–72.
64. Alter BP, Baerlocher GM, Savage SA, Chanock SJ, Weksler BB, Willner JP, et al. Very short telomere length by flow fluorescence in situ hybridization identifies patients with dyskeratosis congenita. Blood. 2007;110:1439–47.
65. Calado RT, Yewdell WT, Wilkerson KL, Regal JA, Kajigaya S, Stratakis CA, et al. Sex hormones, acting on the TERT gene, increase telomerase activity in human primary hematopoietic cells. Blood. 2009;114:2236–43.
66. Alter BP, Gardner FH, Hall RE. Treatment of dyskeratosis congenita with granulocyte colony-stimulating factor and erythropoietin. Br J Haematol. 1997;97:309–11.
67. Giri N, Pitel PA, Green D, Alter BP. Splenic peliosis and rupture in patients with dyskeratosis congenita on androgens and granulocyte colony-stimulating factor. Br J Haematol. 2007;138:815–7.
68. Alter BP, Giri N, Savage SA, Rosenberg PS. Cancer in dyskeratosis congenita. Blood. 2009;113:6549–57.
69. de la Fuente J, Dokal I. Dyskeratosis congenita: advances in the understanding of the telomerase defect and the role of stem cell transplantation. Pediatr Transpl. 2007;11:584–94.
70. Dietz AC, Orchard PJ, Baker KS, Giller RH, Savage SA, Alter BP, et al. Disease-specific hematopoietic cell transplantation: nonmyeloablative conditioning regimen for dyskeratosis congenita. Bone Marrow Transpl. 2011;46:98–104.
71. Nishio N, Takahashi Y, Ohashi H, Doisaki S, Muramatsu H, Hama A, Shimada A, Yagasaki H, Kojima S. Reduced-intensity conditioning for alternative donor hematopoietic stem cell transplantation in patients with dyskeratosis congenita. Pediatr Transpl. 2011;15:161–6.
72. Agarwal S, Loh YH, McLoughlin EM, Huang J, Park IH, Miller JD, et al. Telomere elongation in induced pluripotent stem cells from dyskeratosis congenita patients. Nature. 2010;464:292–6.

Extensive gene deletions in Japanese patients with Diamond-Blackfan anemia

Madoka Kuramitsu,[1] Aiko Sato-Otsubo,[2] Tomohiro Morio,[3] Masatoshi Takagi,[3] Tsutomu Toki,[4] Kiminori Terui,[4] RuNan Wang,[4] Hitoshi Kanno,[5] Shouichi Ohga,[6] Akira Ohara,[7] Seiji Kojima,[8] Toshiyuki Kitoh,[9] Kumiko Goi,[10] Kazuko Kudo,[11] Tadashi Matsubayashi,[12] Nobuo Mizue,[13] Michio Ozeki,[14] Atsuko Masumi,[1] Haruka Momose,[1] Kazuya Takizawa,[1] Takuo Mizukami,[1] Kazunari Yamaguchi,[1] Seishi Ogawa,[2] Etsuro Ito,[4] and Isao Hamaguchi[1]

[1]Department of Safety Research on Blood and Biological Products, National Institute of Infectious Diseases, Tokyo, Japan; [2]Cancer Genomics Project, Graduate School of Medicine, The University of Tokyo, Tokyo, Japan; [3]Department of Pediatrics and Developmental Biology, Graduate School of Medicine, Tokyo Medical and Dental University, Bunkyo-ku, Tokyo, Japan; [4]Department of Pediatrics, Hirosaki University Graduate School of Medicine, Hirosaki, Japan; [5]Department of Transfusion Medicine and Cell Processing, Tokyo Women's Medical University, Tokyo, Japan; [6]Department of Pediatrics, Graduate School of Medical Sciences, Kyushu University, Fukuoka, Japan; [7]First Department of Pediatrics, Toho University School of Medicine, Tokyo, Japan; [8]Department of Pediatrics, Nagoya University Graduate School of Medicine, Nagoya, Japan; [9]Department of Hematology/Oncology, Shiga Medical Center for Children, Shiga, Japan; [10]Department of Pediatrics, School of Medicine, University of Yamanashi, Yamanashi, Japan; [11]Division of Hematology and Oncology, Shizuoka Children's Hospital, Shizuoka, Japan; [12]Department of Pediatrics, Seirei Hamamatsu General Hospital, Shizuoka, Japan; [13]Department of Pediatrics, Kushiro City General Hospital, Hokkaido, Japan; and [14]Department of Pediatrics, Graduate School of Medicine, Gifu University, Gifu, Japan

Fifty percent of Diamond-Blackfan anemia (DBA) patients possess mutations in genes coding for ribosomal proteins (RPs). To identify new mutations, we investigated large deletions in the RP genes *RPL5*, *RPL11*, *RPL35A*, *RPS7*, *RPS10*, *RPS17*, *RPS19*, *RPS24*, and *RPS26*. We developed an easy method based on quantitative-PCR in which the threshold cycle correlates to gene copy number. Using this approach, we were able to diagnose 7 of 27 Japanese patients (25.9%) possessing mutations that were not detected by sequencing. Among these large deletions, similar results were obtained with 6 of 7 patients screened with a single nucleotide polymorphism array. We found an extensive intragenic deletion in *RPS19*, including exons 1-3. We also found 1 proband with an *RPL5* deletion, 1 patient with an *RPL35A* deletion, 3 with *RPS17* deletions, and 1 with an *RPS19* deletion. In particular, the large deletions in the *RPL5* and *RPS17* alleles are novel. All patients with a large deletion had a growth retardation phenotype. Our data suggest that large deletions in RP genes comprise a sizable fraction of DBA patients in Japan. In addition, our novel approach may become a useful tool for screening gene copy numbers of known DBA genes. (*Blood*. 2012;119(10): 2376-2384)

Introduction

Diamond-Blackfan anemia (DBA; MIN# 105650) is a rare congenital anemia that belongs to the inherited BM failure syndromes, generally presenting in the first year of life. Patients typically present with a decreased number of erythroid progenitors in their BM.[1] A main feature of the disease is red cell aplasia, but approximately half of patients show growth retardation and congenital malformations in the craniofacial, upper limb, cardiac, and urinary systems. Predisposition to cancer, in particular acute myeloid leukemia and osteogenic sarcoma, is also characteristic of the disease.[2]

Mutations in the *RPS19* gene were first reported in 25% of DBA patients by Draptchinskaia et al in 1999.[3] Since that initial finding, many genes that encode large (RPL) or small (RPS) ribosomal subunit proteins were found to be mutated in DBA patients, including *RPL5* (approximately 21%), *RPL11* (approximately 9.3%), *RPL35A* (3.5%), *RPS7* (1%), *RPS10* (6.4%), *RPS17* (1%), *RPS24* (2%), and *RPS26* (2.6%).[4-7] To date, approximately half of the DBA patients analyzed have had a mutation in one of these genes. Konno et al screened 49 Japanese patients and found that 30% (12 of 49) carried mutations.[8] In addition, our data showed that 22 of 68 DBA patients (32.4%) harbored a mutation in ribosomal protein (RP) genes (T.T., K.T., R.W., and E.I., unpublished observation, April 16, 2011). These abnormalities of RP genes cause defects in ribosomal RNA processing, formation of either the large or small ribosome subunit, and decreased levels of polysome formation,[4-6,9-12] which is thought to be one of the mechanisms for impairment of erythroid lineage differentiation.

Although sequence analyses of genes responsible for DBA are well established and have been used to identify new mutations, it is estimated that approximately half of the mutations remain to be determined. Because of the difficulty of investigating whole allele deletions, there have been few reports regarding allelic loss in DBA, and they have only been reported for *RPS19* and *RPL35A*.[3,6,13] However, a certain percentage of DBA patients are thought to have a large deletion in RP genes. Therefore, a detailed analysis of allelic loss mutations should be conducted to determine other RP genes that might be responsible for DBA.

In the present study, we investigated large deletions using our novel approach for gene copy number variation analysis based on quantitative-PCR and a single nucleotide polymorphism (SNP) array. We screened Japanese DBA patients and found 7 patients with a large deletion in an allele in *RPL5*, *RPL35A*, *RPS17*, or *RPS19*. Interestingly, all of these patients with a large deletion had a phenotype of growth retardation, including short stature and

Submitted July 24, 2011; accepted November 15, 2011. Prepublished online as *Blood* First Edition paper, January 18, 2012; DOI 10.1182/blood-2011-07-368662.

The online version of this article contains a data supplement.

The publication costs of this article were defrayed in part by page charge payment. Therefore, and solely to indicate this fact, this article is hereby marked "advertisement" in accordance with 18 USC section 1734.

Table 1. Primers used for synchronized quantitative-PCR (s-q-PCR) of RPL proteins

Gene	Primer name	Sequence	Primer name	Sequence	Size, bp
RPL5	L5-02F	CTCCCAAAGTGCTTGAGATTACAG	L5-02R	CACCTTTTCCTAACAAATTCCCAAT	132
	L5-05F	AGCCCTCCAACCTAGGTGACA	L5-05R	GAATTGGGATGGGCAAGAACT	102
	L5-17F	TGAACCCTTGCCCTAAAACATG	L5-17R	TCTTGGTCAGGCCCTGCTTA	105
	L5-19F	ATTGTGCAAACTCGATCACTAGCT	L5-19R	GTGTCTGAGGCTAACACATTTCCAT	103
	L5-21F	GTGCCACTCTCTTGGACAAACTG	L5-21R	CATAGGGCCAAAAGTCAAATAGAAG	102
	L5-28F	TCCACTTTAGGTAGGCGAAACC	L5-28R	TCAGATTTGGCATGTACCTTTCA	102
RPL11	L11-06F	GCACCCACATGGCTTAAAGG	L11-6R	CAACCAACCCATAGGCCAAA	102
	L11-20F	GAGCCCCCTTTCTCAGATGATA	L11-20R	CATGAACTTGGGCTCTGAATCC	109
	L11-22F	TATGTGCAGATAAGAGGGCAGTCT	L11-22R	ATACAGATAAGGAAACTGAGGCAGATT	98
RPL19	L19-02F	TGGCCTCTCATAAAGGAAATCTCT	L19-02R	GGAATGCAGGCAAGTTACTCTGTT	103
	L19-08F	TTTGAAGGCAAGAAATAAGTTCCA	L19-08R	AGCACATCACAGAGTCCAAATAGG	107
	L19-16F	GGTTAGTTGAAGCAGGAGCCTTT	L19-16R	TGCTAGGGAGACAGAAGCACATC	102
	L19-19F	GGACCAGTAGTTGTGACATCAGTTAAG	L19-19R	CCCATTTGTAACCCCCACTTG	106
RPL26	L26-03F	TCCAAAGAGCTGAGACAGAAGTACA	L26-03R	TCCATCAAGACAACGAGAACAAGT	102
	L26-16F	TTTGAGAATGCTTGAGAGAAGGAA	L26-16R	TTCCAGCACATGTAAAATCAAGGA	102
	L26-18F	ATGTTTTAATAAGCCCTCCAGTTGA	L26-18R	GAGAACAGCAAGTTGAAAGGTTCA	102
	L26-20F	GGGCTTTGCTTGATCACTCTAGA	L26-20R	AGGGAGCCCGAAAACATTTAC	104
RPL35A	L35A-01F	TGTGGCTTCTATTTTGCGTCAT	L35A-01R	GGAATTACCTCCTTTATTGCTTACAAG	121
	L35A-07F	TTTCCGTTCTGTCTATTGCTGTGT	L35A-07R	GAACCCTGAGTGGAGGATGTTC	113
	L35A-17F	GCCCACAACCTCCAGAGAATC	L35A-17R	GGATCACTTGAGGCCAGGAAT	104
	L35A-18F	TTAGGTGGGCTTTTCAGTCTCAA	L35A-18R	ATCTCCTGATTCCCCAACTTTGT	102
RPL36	L36-02F	CCGCTCTACAAGTGAAGAAATTCTG	L36-02R	CTCCCTCTGCCTGTGAAATGA	102
	L36-04F	TGCGTCCTGCCAGTGTTG	L36-04R	GGGTAGCTGTGAGAACCAAGGT	105
	L36-17F	CCCCTTGAAAGGACAGCAGTT	L36-17R	TTGGACACCAGGCACAGACTT	114

Table 2. Primers used for s-q-PCR of RPS proteins

Gene	Primer name	Sequence	Primer name	Sequence	Size, bps
RPS7	S7-11F	GCGCTGCCAGATAGGAAATC	S7-11R	TTAGGGAGCTGCCTTACATATGG	102
	S7-12F	ACTGGCAGTTCTGTGATGCTAAGT	S7-12R	ACTCTTGCTCATCTCCAAAACCA	102
	S7-16F	GTGTCTGTGCCAGAAAGCTTGA	S7-16R	GAACCATGCAAAAGTGCCAATAT	112
RPS10	S10-03F	CTACGGTTTTGTGTGGGTCACTT	S10-03R	CATCTGCAAGAAGGAGACGATTG	102
	S10-15F	GTTGGCCTGGAGTCGTGATTT	S10-15R	ATTCCAAGTGCACCATTTCCTT	101
	S10-17F	AATGGTGTTTAGGCCAACGTTAC	S10-17R	TTTGAACAGTGGTTTTTGTGCAT	100
RPS14	S14-03F	GAATTCCAAACCCTTCTGCAAA	S14-03R	TTGCTTCATTTACTCCTCAAGACATT	104
	S14-05F	ACAACCAGCCCTCTACCTCTTTT	S14-05R	GGAAGACGCCGGCATTATT	102
	S14-06F	CGCCTCTACCTCGCCAAAC	S14-06R	GGGATCGGTGCTATTGTTATTCC	102
	S14-09F	GCCATCATGCCGAAACATACT	S14-09R	AACGCGCCACAGGAGAGA	102
	S14-13F	ATCAGGTGGAGCACAGGAAAAC	S14-13R	GCGAGGGAGCTGCTTGATT	111
	S14-15F	AGAAGTTTTAGTGAGGCAGAAATGAGA	S14-15R	TCCCCTGGCTATTAAATGAAACC	102
	S14-19F	GATGAATTGTCCTTTCCTCCATTC	S14-19R	TAGGCGGAAACCAAAAATGCT	102
RPS15	S15-11F	CTCAGCTAATAAAGGCGCACATG	S15-11R	CCTCACACCACGAACCTGAAG	108
	S15-15F	GGTTGGAGAACATGGTGAGAACTA	S15-15R	CACATCCCTGGGCCACTCT	108
RPS17	S17-03F	ACTGCTGTCGTGGCTCGATT	S17-03R	GATGACCTGTTCTTCTGGCCTTA	121
	S17-05F	GAAAACAGATACAAATGGCATGGT	S17-05R	TGCCTCCCACTTTTCCAGAGT	114
	S17-12F	CTATGTGTAGGAGGTCCCAGGATAG	S17-12R	CCACCTGGTACTGAGCACATGT	102
	S17-16F	TAGCGGAAGTTGTGTGCATTG	S17-16R	CAAGAACAGAAGCAGCCAAGAG	102
	S17-18F	TGGCTGAATCTGCCTGCTT	S17-18R	GCCTTGTATGTACCTGGAAATGG	103
	S17-20F	GGGCCCTTCACAAATGTTGA	S17-20R	GCAAAACTCTGTCCCTTTGAGAA	101
RPS19	S19-24F	CCATCCCAAGAATGCACACA	S19-24R	CGCCGTAGCTGGTACTCATG	120
	S19-28F	GACACACCTGTTGAGTCCTCAGAGT	S19-28R	GCTTCTATTAACTGGAGCACACATCT	114
	S19-36F	CTCTTGAGGGTGGTCTGGAAAT	S19-36R	GTCTTTGCGGGTTCTTCCTCTAC	102
	S19-40F	GGAACGGTGTCAGGATTCAAG	S19-40R	AGCGGCTGTACACCAGAAATG	101
	S19-44F	CTGAGGTTGAGTGTCCCATTTCT	S19-44R	GCACCGGGCCTCTGTTATC	104
	S19-57F	CAGGGACACAGTGCTGAGAAACT	S19-57R	TGAGATGTCCCATTTTCACTATTGTT	101
	S19-58F	CATGATGTTAGCTCCGTTGCATA	S19-58R	ATTTTGGGAAGAGTGAAGCTTAGGT	102
	S19-62F	GCAACAGAGCGAGACTCCATTT	S19-62R	AGCACTTTTCGGCACTTACTTCA	102
	S19-65F	ACATTTCCCAGAGCTGACATGA	S19-65R	TCGGGACACCTAGACCTTGCT	102
RPS24	S24-17F	CGACCACGTCTGGCTTAGAGT	S24-17R	CCTTCATGCCCAACCAAGTC	101
	S24-20F	ACAAGTAAGCATCATCACCTCGAA	S24-20R	TTTCCCTCACAGCTATCGTATGG	105
	S24-32F	GGGAAATGCTGTGTCCACATACT	S24-32R	CTGGTTTCATGGCTCCAGAGA	105
RPS26	S26-03F	CGCAGCAGTCAGGGACATTT	S26-03R	AAGTTGGGCGAAGGCTTTAAG	104
	S26-05F	ATGGAGGCCGTCTAGTTTGGT	S26-05R	TGCCTACCCTGAACCTTGCT	102
RPS27A	S27A-09F	GCTGGAGTGCATTCGCTTGT	S27A-09R	CACGCCTGTAATCCCCACTAA	102
	S27A-12F	CAGGCTTGGTGTGCTGTGACT	S27A-12R	ACGTCCATCTTCCAGCTGCTT	103
	S27A-18F	GGGTTTTTCCTGTTTGGTATTTGA	S27A-18R	AAAGGCCAGCTTTGCAAGTG	111
	S27A-22F	TTACCATATTGCCAGTCTTTCCATT	S27A-22R	TTCATATGCATTTGCACAAACTGT	106

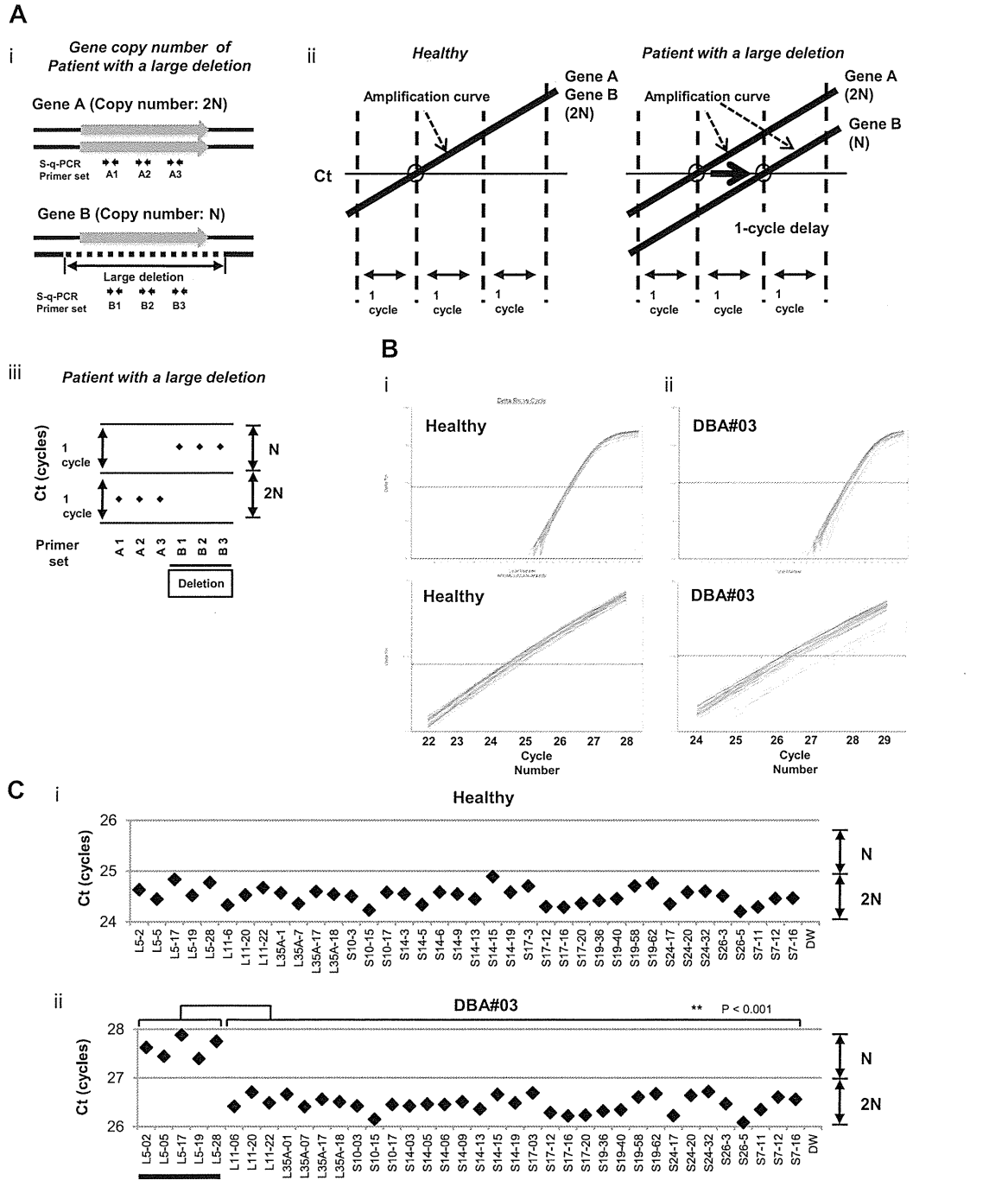

Figure 1. s-q-PCR can determine a large gene deletion in DBA. (A) Concept of the DBA s-q-PCR assay. The difference in gene copy number between a healthy sample and that with a large deletion is 2-fold (i). When all genomic s-q-PCR for genes of interest synchronously amplify DNA fragments, a 2-fold difference in the gene copy number is detected by a 1-cycle difference of the Ct scores of the s-q-PCR amplification curves (ii). Also shown is a dot plot of the Ct scores (iii). (B) Results of the amplification curves of s-q-PCR performed with a healthy person (i) and a DBA patient (patient 3; ii). The top panel shows the results of PCR cycles; the bottom panel is an extended graph of the PCR cycles at logarithmic amplification. (C) Graph showing Ct scores of s-q-PCR. If all specific primer sets for DBA genes show a 1-cycle delay relative to each other, this indicates a large deletion in the gene. Gene primer sets with a large deletion are underlined in the graph. $^{**}P < .001$.

small-for-gestational age (SGA), which suggests that this is a characteristic of DBA patients with a large gene deletion in Japan.

Methods

Patient samples

Genomic DNA was extracted using the GenElute Blood Genomic DNA Kit (Sigma-Aldrich) according to the manufacturer's protocol. Clinical manifestation of patients from a Japanese DBA genomic library are listed elsewhere or are as reported by Konno et al.[8] The study was approved by the institutional review board at the National Institute of Infectious Diseases and Hirosaki University.

DBA gene copy number assay by s-q-PCR

For s-q-PCR, primers were designed using Primer Express Version 3.0 software (Applied Biosystems). Primers are listed in Tables 1 and 2. Genomic DNA in water was denatured at 95°C for 5 minutes and

immediately cooled on ice. The composition of the s-q-PCR mixture was as follows: 5 ng of denatured genomic DNA, 0.4mM forward and reverse primers, 1× SYBR Premix Ex Taq II (Takara), and 1× ROX reference dye II (Takara) in a total volume of 20 μL (all experiments were performed in duplicate). Thermal cycling was performed using the Applied Biosystems 7500 fast real-time PCR system. Briefly, the PCR mixture was denatured at 95°C for 30 seconds, followed by 35 cycles of 95°C for 5 seconds, 60°C for 34 seconds, and then dissociation curve measurement. Threshold cycle (Ct) scores were determined as the average of duplicate samples. The technical errors of Ct scores in the triplicate analysis were within 0.2 cycles (supplemental Figure 1, available on the *Blood* Web site; see the Supplemental Materials link at the top of the online article). The sensitivity and specificity of this method was evaluated with 15 healthy samples. Any false positive was not observed in all primer sets in all healthy samples (supplemental Figure 2). We performed direct sequencing of the s-q-PCR products. The results of the sequence analysis were searched for using BLAST to confirm uniqueness. Sequence data were obtained from GenBank (http://www.ncbi.nlm.nih.gov/gene/) and Ensemble Genome Browser (http://uswest.ensembl.org).

Genomic PCR

Genomic PCR was performed using KOD FX (Toyobo) according to the manufacturer's step-down PCR protocol. Briefly, the PCR mixture contained 20 ng of genomic DNA, 0.4mM forward and reverse primers, 1mM dNTP, 1× KOD FX buffer, and 0.5 U KOD FX in a total volume of 25 μL in duplicate. Primers are given in supplemental Figure 3 and Table 2. PCR mixtures were denatured at 94°C for 2 minutes, followed by 4 cycles of 98°C for 10 seconds, 74°C for 12 minutes, followed by 4 cycles of 98°C for 10 seconds, 72°C for 12 minutes followed by 4 cycles of 98°C for 10 seconds, 70°C for 12 minutes, followed by 23 cycles of 98°C for 10 seconds and 68°C for 12 minutes. PCR products were loaded on 0.8% agarose gels and detected by LAS-3000 (Fujifilm).

DNA sequencing analysis

The genomic PCR product was purified by the GenElute PCR clean-up kit (Sigma-Aldrich) according to the manufacturer's instructions. Direct sequencing was performed using the BigDye Version 3 sequencing kit. Sequences were read and analyzed using a 3120x genetic analyzer (Applied Biosystems).

SNP array-based copy number analysis

SNP array experiments were performed according to the standard protocol of GeneChip Human Mapping 250K Nsp arrays (Affymetrix). Microarray data were analyzed for determination of the allelic-specific copy number using the CNAG program, as described previously.[14] All microarray data are available at the EGA database (www.ebi.ac.uk/ega) under accession number EGAS00000000105.

Results

Construction of a convenient method for RP gene copy number analysis based on s-q-PCR

We focused on the heterozygous large deletions in DBA-responsible gene. The difference in copy number of genes between a mutated DBA allele and the intact allele was 2-fold (N and 2N; Figure 1Ai). If each PCR can synchronously amplify DNA fragments when the template genomic DNA used is of normal karyotype, it is possible to conveniently detect a gene deletion with a 1-cycle delay in s-q-PCR analysis (Figure 1Aii-iii).

Table 3. Summary of mutations and the mutation rate observed in Japanese DBA patients

Gene	Sequencing analysis
RPS19	10
RPL5	6
RPL11	3
RPS17	1
RPS10	1
RPS26	1
RPL35A	0
RPS24	0
RPS14	0
Mutations, n (%)	22 (32.4%)
Total analyzed, N	68

To apply this strategy for allelic analysis of DBA, we prepared primers for 16 target genes, *RPL5*, *RPL11*, *RPL35A*, *RPS10*, *RPS19*, *RPS26*, *RPS7*, *RPS17*, *RPS24*, *RPL9*, *RPL19*, *RPL26*, *RPL36*, *RPS14*, *RPS15*, and *RPS27A*, under conditions in which the Ct of s-q-PCR would occur within 1 cycle of that of the other primer sets (Tables 1 and 2). At the same time, we defined the criteria of a large deletion in our assay as follows. If multiple primer sets for one gene showed a 1-cycle delay from the other gene-specific primer set at the Ct score, we assumed that this represented a large deletion. As shown in Figure 1Bii and 1Cii, the specific primer sets for *RPL5* (L5-02, L5-05, L5-17, L5-19, and L5-28) detected a 1-cycle delay with respect to the mutated allele of patient 3. This assessment could be verified by simply confirming the difference of the cycles with the s-q-PCR amplification curves.

Study of large gene deletions in a Japanese DBA genomic DNA library

Sixty-eight Japanese DBA patients were registered and blood genomic DNA was collected at Hirosaki University. All samples were first screened for mutations in *RPL5*, *L11*, *L35A*, *S10*, *S14*, *S17*, *S19*, and *S26* by sequencing. Among these patients, 32.4% (22 of 68) had specific DBA mutations (Table 3 and data not shown). We then screened for large gene deletions in 27 patients from the remaining 46 patients who did not possess mutations as determined by sequencing (Table 4).

When we performed the s-q-PCR DBA gene copy number assay, 7 of 27 samples displayed a 1-cycle delay of Ct scores: 1 patient had *RPL5* (patient 14), 1 had *RPL35A* (patient 71), 3 had *RPS17* (patients 3, 60, 62), and 2 had *RPS19* (patients 24 and 72; Figure 2 and Table 4). Among these patients, the large deletions in the *RPL5* and *RPS17* genes are the first reported cases of allelic deletions in DBA. From these results, we estimate that a sizable number of Japanese DBA patients have a large deletion.

Based on our findings, the rate of large deletions was approximately 25.9% (7 of 27) in a category of unspecified gene mutations. Such mutations have typically gone undetected by conventional sequence analysis. We could not find any additional gene deletions in the analyzed samples.

Confirmation of the gene copy number for DBA genes by genome-wide SNP array

We performed genome-wide copy number analysis of the 27 DBA patients with a SNP array to confirm our s-q-PCR results. SNP array showed that patient 3 had a large deletion in

Table 4. Characteristics of DBA patients tested

Patient no.	Age at diagnosis	Sex	Hb, g/dL	Large deletion by s-q-PCR	Large deletion by SNP array	Inheritance	Malformations	Response to first steroid therapy
Patients with a large deletion in RP genes								
3*†	1 y	M		RPL5	RPL5	Sporadic	Short stature, thumb anomalies	Response
14*	5 y	M	5.5	RPS17	RPS17	Sporadic	White spots, short stature	Response
24*†	1 mo	F	5.5	RPS19	ND	Sporadic	Short stature, SGA	Response
60*†	2 mo	F	2.4	RPS17	RPS17	Sporadic	SGA	NT
62*†	1 mo	F	6.2	RPS17	RPS17	Sporadic	Small ASD, short stature, SGA	Response
71	0 y	M	5.3	RPL35A	RPL35A	Sporadic	Thumb anomalies, synostosis of radius and ulna, Cohelia Lange-like face, cleft palate, underdescended testis, short stature, cerebellar hypoplasia, fetal hydrops	NT
72†	0 y	M	2	RPS19	RPS19	Sporadic	Thumb anomalies, flat thenar, testicular hypoplasia, fetal hydrops, short stature, learning disability	No
Patients without a large deletion in RP genes								
5*	1 y	F	3.1	ND	ND	Sporadic	ND	Response
15*	1 mo	F	1.6	ND	ND	Sporadic	ND	Response
21*	1 y	F	2.6	ND	ND	Sporadic	ND	Response
26*	1 y 1 mo	F	8	ND	ND	Sporadic	Congenital hip dislocation, spastic quadriplegia, hypertelorism, nystagmus, short stature, learning disability	Response
33*	2 mo	F	1.3	ND	ND	Sporadic	ND	Response
36*	0 y	M	8.2	ND	ND	Familial	ND	Response
37*	4 y	M	6.1	ND	ND	Sporadic	Hypospadias, underdescended testis, SGA	NT
45*	5 d	M	5.1	ND	ND	Sporadic	Short stature, microcephaly, mental retardation, hypogammaglobulinemia	Poor
50*	2 m	F	3.4	ND	ND	Familial	ND	Response
61*	9 m	M	4	ND	ND	Sporadic	ND	Response
63*	0 y	M	6.8	ND	ND	Sporadic	Micrognathia, hypertelorism, short stature	Response
68	1 y 4 mo	M	5.9	ND	ND	Sporadic	ND	NT (CR)
69	1 y	M	9.3	ND	ND	Sporadic	ND	Response
76	0 y	M	4	ND	ND	Sporadic	ND	Response
77	0 y	M	7.8	ND	ND	Familial	Short stature	No
83	9 mo	F	3	ND	ND	Sporadic	ND	NT
90	10 mo	M	9	ND	ND	Sporadic	ND	No
91	0 y	F	3.8	ND	ND	Sporadic	ND	Response
92	2 mo	M	3.7	ND	ND	Sporadic	ASD, PFO, melanosis, underdescended testis, SGA, short stature	Response
93	11 mo	M	2.2	ND	ND	Sporadic	White spots, senile face, corneal opacity, underdescended testis, syndactyly, ectrodactyly, flexion contracture, extension contracture	Response

ND indicates not detected; NT, not tested; CR, complete remission; ASD, atrial septal defect; and PFO, persistent foramen ovale.

*Status data of Japanese probands 3 to 63 is from a report by Konno et al.[8]

†Large deletions of the parents of 5 DBA patients (3, 24, 60, 62, and 72) were analyzed by s-q-PCR, but there were no deletions in DBA genes in any of the 5 pairs of parents.

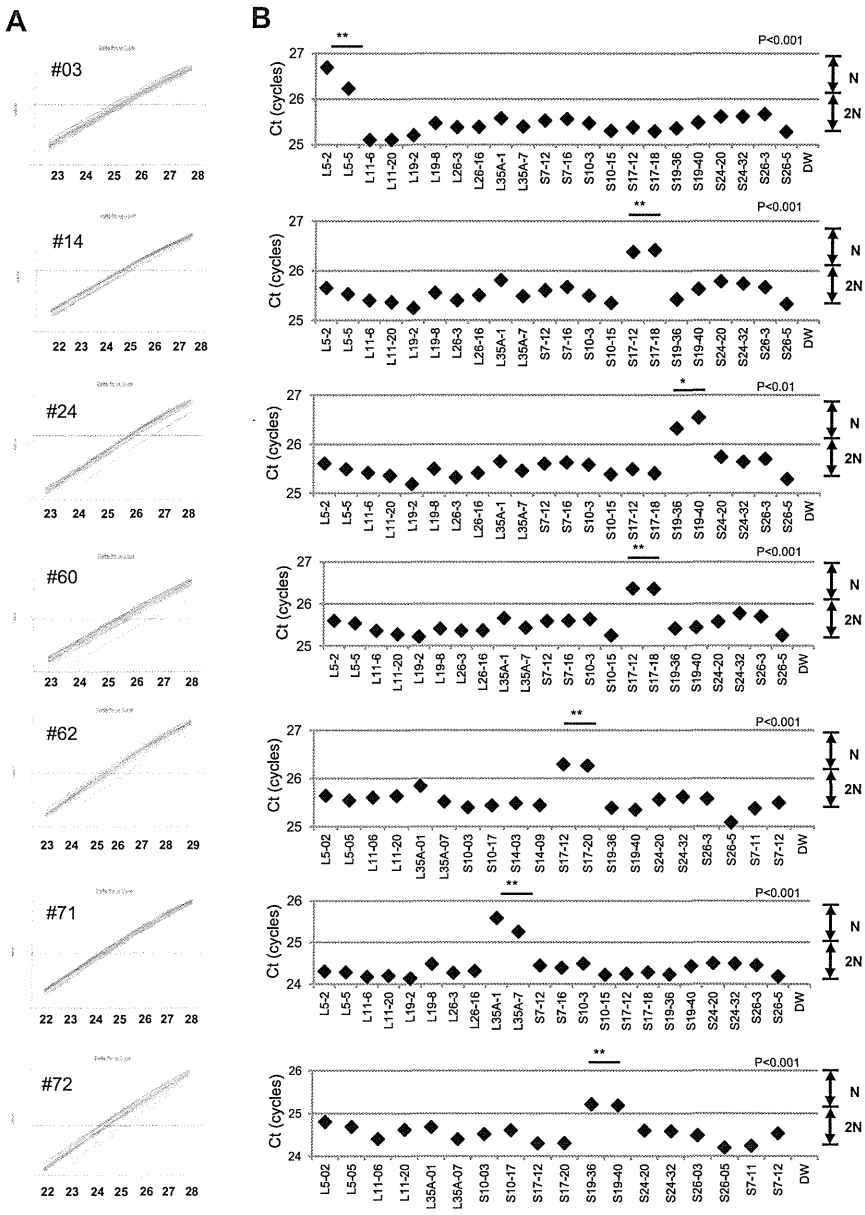

Figure 2. Detection of 7 mutations with a large deletion in DBA patients. Genomic DNA of 27 Japanese DBA patients with unknown mutations were subjected to the DBA gene copy number assay. (A) Amplification curve of s-q-PCR of a mutation with a large deletion. The deleted gene can be easily distinguished. (B) Ct score (cycles) of representative s-q-PCR with DBA genomic s-q-PCR primers. Results of the 2 gene-specific primer pairs indicated in the graph are representative of at least 2 sets for each gene-specific primer (carried out in the same run). $^{**}P < .001$; $^{*}P < .01$

chromosome 1 (ch1) spanning 858 kb (Figure 3A); patient 71 had a large deletion in ch3 spanning 786 kb (Figure 3B); patients 14, 60, and 62 had a large deletion in ch15 spanning 270 kb, 260 kb, and 330 kb, respectively (Figure 3C); and patient 72 had a large deletion in ch19 spanning 824 kb (Figure 3D). However, there were no deletions detected in ch19 in patient 24 (Figure 3D). Genes estimated to reside within a large deletion are listed in supplemental Table 1. Consistent with these s-q-PCR results, 6 of 7 large deletions were detected and confirmed as deleted regions, and these large deletions contained *RPL5*, *RPL35A*, *RPS17*, and *RPS19* (Table 4 and supplemental Table 1). Other large deletions in RP genes were not detected by this analysis. From these results, we conclude that the synchronized multiple PCR amplification method has a detection sensitivity comparable to that of SNP arrays.

Detailed examination of a patient with intragenic deletion in the RPS19 allele (patient 24)

Interestingly, for patient 24, in whom we could not detect a large deletion by SNP array at s-q-PCR gene copy number analysis, 2 primer sets for *RPS19* showed a 1-cycle delay (RPS19-36 and RPS19-40), but 2 other primer pairs (RPS19-58 and RPS19-62) did not show this delay (Figure 4A). We attempted to determine the deleted region in detail by testing more primer sets on *RPS19*. We tested a total of 9 primer sets for *RPS19* (Figure 4B) and examined the gene copy numbers. Surprisingly, 4 primer sets (S19-24, S19-36, S19-40, and S19-44) for intron 3 of *RPS19* indicated a 1-cycle delay, but the other primers for *RPS19* located on the 5′untranslated region (5′UTR), intron 3, or 3′UTR did not show this delay (S19-57, S19-58, S19-28, S19-62, and S19-65; Figure 4B-C). These results suggest that the intragenic deletion occurred in the *RPS19* allele. To confirm this deleted region precisely, we performed genomic PCR on *RPS19*, amplifying a region from the 5′UTR to intron 3 (Figure

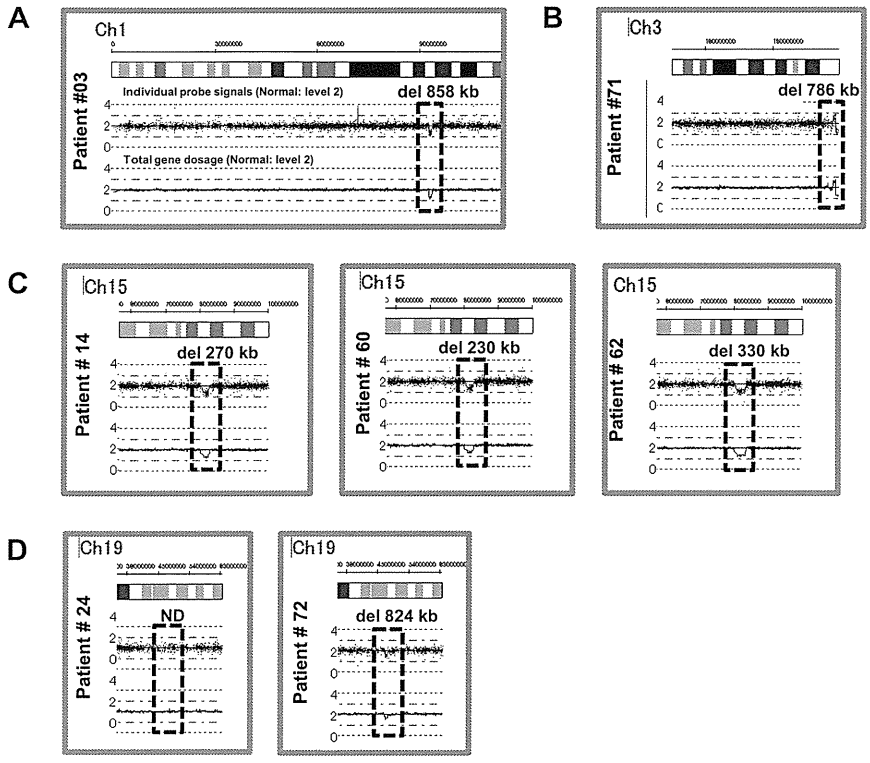

Figure 3. Results of SNP genomic microarray (SNP-chip) analysis. Genomic DNA of 27 Japanese DBA patients with unknown mutations was examined using a SNP array. Six patients had large deletions in their chromosome (ch), which included one DBA-responsible gene. Patient 3 has a large deletion in ch1 (A), patient 71 has a deletion in ch3 (B), patients 14, 60, and 62 have deletions in ch15 (C), and patient 72 has a deletion in ch19 (D).

4B). In patient 24, we observed an abnormally sized PCR product at a low molecular weight by agarose gel electrophoresis (Figure 4D). We did not detect a wild-type PCR product from the genomic PCR. This finding is probably because PCR tends to amplify smaller molecules more easily. However, we did detect a PCR fragment at the correct size using primers located in the supposedly deleted region. These bands were thought to be from the products of a wild-type allele. Sequencing of the mutant band revealed that intragenic recombination occurred at a homologous region of 27 nucleotides, from −1400 to −1374 in the 5′ region, to +5758 and +5784 in intron 3, which resulted in the loss of 7157 base pairs in the *RPS19* gene (Figure 4E). The deleted region contains exons 1, 2, and 3, and therefore the correct *RPS19* mRNA could not be transcribed.

Genotype-phenotype analysis and DBA mutations in Japan

Patients with a large deletion in DBA genes had common phenotypes (Table 4). Malformation with growth retardation (GR), including short stature or SGA, were observed in all 7 patients. In patients who had a mutation found by sequencing, half had GR (11 of 22; status data of DBA patients with mutations found by sequencing are not shown). GR may be a distinct phenotypic feature of large deletion mutations in Japanese DBA patients. Familial mutations were analyzed for parents for 5 DBA patients with a large deletion (patients 3, 24, 60, 62, and 72) by s-q-PCR. There are no large deletions in all 5 pairs of parents in DBA-responsible genes. Four of the 7 patients responded to steroid therapy. We have not observed significant phenotypic differences between patients with extensive deletions and other patients with regard to blood counts, responsiveness to treatment, or other malformations.

Discussion

Many studies have reported RP genes to be responsible for DBA. However, mutations have not been determined for approximately half of DBA patients analyzed. There are 2 possible reasons for this finding. One possibility is that patients have other genes responsible for DBA, and the other is that patients have a complicated set of mutations in RP genes that are difficult to detect. In the present study, we focused on the latter possibility because we have found fewer Japanese DBA patients with RP gene mutations (32.4%) compared with another cohort study of 117 DBA patients and 9 RP genes (approximately 52.9%).[4] With our newly developed method, we identified 7 new mutations with a large deletion in *RPL5*, *RPL35A*, *RPS17*, and *RPS19*.

The frequency of a large deletion was approximately 25.9% (7 of 27) in our group of patients who were not found to have mutations by genomic sequencing. Therefore, total RP gene mutations were confirmed in 42.6% of these Japanese patients (Table 5). Interestingly, mutations in *RPS17* have been observed at a high rate (5.9%) in Japan relative to that in other countries (1%).[5,15,16] Although the percentage of DBA mutations differs among different ethnic groups,[8,17-19] a certain portion of large deletions in DBA-responsible genes are likely to be determined in other countries by new strategies.

In the present study, we analyzed patient data to determine genotype-phenotype relations. To date, large deletions have been reported with RPS19 and RPL35A in DBA patients.[3,6,13] *RPS19* large deletions/translocations have been reported in 12 patients, and *RPL35A* large deletions have been reported in 2 patients.[19] GR in patients with a large deletion has been observed previously with *RPS19* translocations,[3,19-21] but it was not found in 2 patients with *RPL35A* deletion.[6] Interestingly, all of our patients with a large deletion had a phenotype

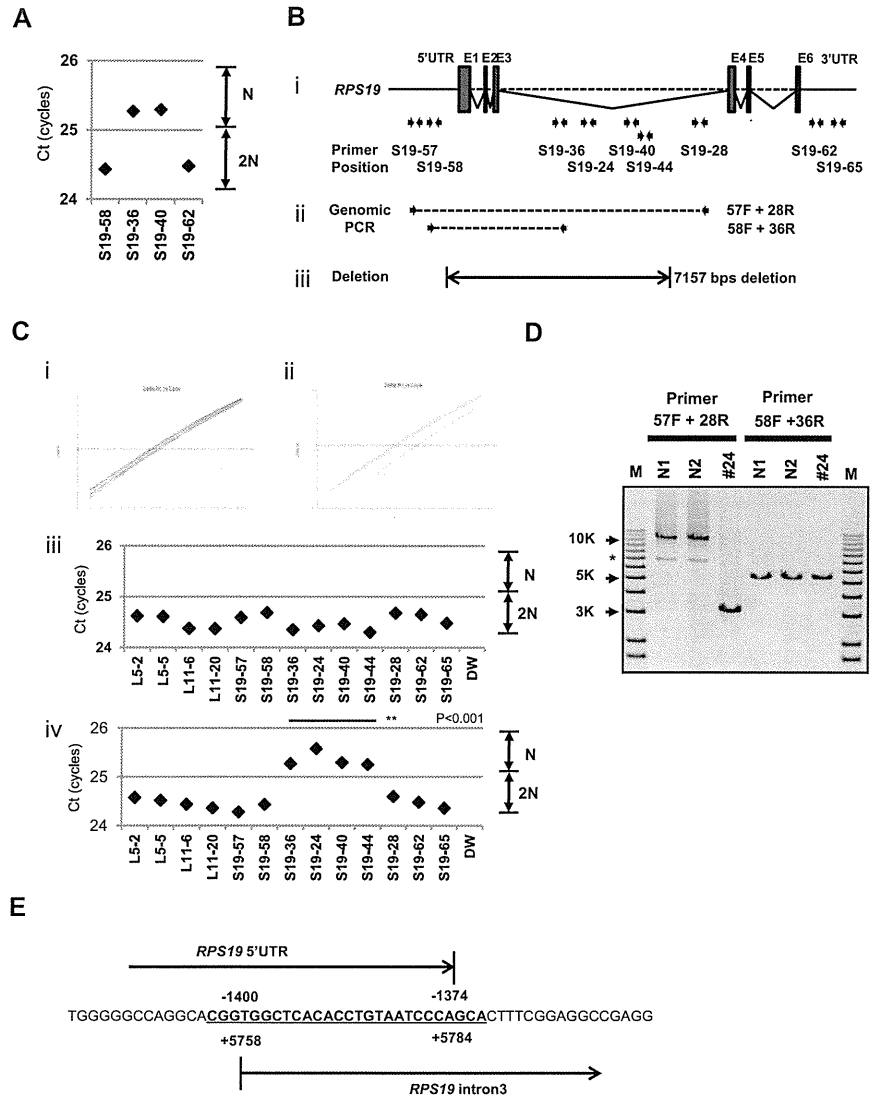

Figure 4. Result of s-q-PCR gene copy number assay for patient 24. (A) Results of s-q-PCR gene copy number assay for *RPS19* with 4 primer sets. (Bi) The *RPS19* gene copy number was analyzed with 9 specific primer sets for *RPS19* that span from the 5′UTR to the 3′UTR. (ii) Primer positions of genomic PCR for *RPS19*. (iii) Region determined to be an intragenic deletion in *RPS19*. (C) Results of gene copy number assay for *RPS19* show a healthy person (i,iii) and a DBA patient (ii,iv), and Ct results are shown (iii-iv). Patient 24 showed a "1-cycle delay" with primers located in the intron 3 region, but other primer sets were normal. (D) Results of genomic PCR amplification visualized by agarose gel electrophoresis to determine the region of deletion. N1 and N2 are healthy samples. *Nonspecific band. (E) Results from the genomic sequence of the 3-kb DNA band from genomic PCR on patient 24 showing an intragenic recombination from −1400 to 5784 (7157 nt) in *RPS19*. $^{**}P < .001$.

of GR, including short stature and SGA, which suggests that this is a characteristic of DBA with a large gene deletion in Japan. Our study results suggest the possibility that GR is associated with extensive deletion in Japanese patients. Although further case studies will be needed to confirm this possibility, screening of DBA samples using our newly developed method will help to advance our understanding of the broader implications of the mutations and the correlation with the DBA genotype-phenotype.

Table 5. Total mutations in Japanese DBA patients, including large gene deletions

Gene	Mutation rate
RPS19	12(17.6%)
RPL5	7(10.3%)
RPL11	3 (4.4%)
RPS17	4 (5.9%)
RPS10	1 (1.5%)
RPS26	1 (1.5%)
RPL35A	1 (1.5%)
RPS24	0
RPS14	0
Mutations, n (%)	29(42.6%)
Total analyzed, N	68

Copy number variation analysis of DBA has been performed by linkage analysis, and the *RPS19* gene was first identified as a DBA-susceptibility gene. Comparative genomic hybridization array technology has also been used to detect DBA mutations in *RPL35A*, and multiplex ligation-dependent probe amplification has been used for *RPS19* gene deletion analysis.[3,6,13,22] However, these analyzing systems have problems in mutation screening. Linkage analysis is not a convenient tool to screen for multiple genetic mutations, such as those in DBA, because it requires a high level of proficiency. Although comparative genomic hybridization technology is a powerful tool with which to analyze copy number comprehensively, this method requires highly specialized equipment and analyzing software, which limits accessibility for researchers. Whereas quantitative PCR–based methods for copy number variation analysis are commercially available (TaqMan), they require a standard curve for each primer set, which limits the number of genes that can be loaded on a PCR plate. To address this issue, a new method of analysis is needed. By stringent selection of PCR primers, the s-q-PCR method enables analysis of many DBA genes in 1 PCR plate and the ability to immediately distinguish a large deletion using the s-q-PCR amplification curve. In our study, 6 of 7 large deletions in the RP gene detected by s-q-PCR were confirmed by SNP arrays (Figure 3). Interestingly, we detected

1 large intragenic deletion in *RPS19*, which was not detected by the SNP array. This agreement between detection results suggests that the s-q-PCR copy number assay could be useful for detecting large RP gene deletions.

In the present study, 7 DBA patients carried a large deletion in the RP genes. This type of mutation could be underrepresented by sequencing analysis, although in the future, genome sequencing might provide a universal platform for mutation and deletion detection. We propose that gene copy number analysis for known DBA genes, in addition to direct sequencing, should be performed to search for a novel responsible gene for DBA. Although at present, it may be difficult to observe copy numbers on all 80 ribosomal protein genes in one s-q-PCR assay, our method allows execution of gene copy number assays for several target genes in 1 plate. Because our method is quick, easy, and low cost, it could become a conventional tool for detecting DBA mutations.

Acknowledgments

The authors thank Momoka Tsuruhara, Kumiko Araki, and Keiko Furuhata for their expert assistance.

This work was partially supported by grants-in-aid for scientific research from the Ministry of Education, Culture, Sports, Science and Technology of Japan, and by Health and Labor Sciences research grants (Research on Intractable Diseases) from the Ministry of Health, Labor and Welfare of Japan.

Authorship

Contribution: M.K. designed and performed the research, analyzed the data, and wrote the manuscript; A.S-O. and S. Ogawa performed the SNP array analysis; T.M., M.T., and M.O designed the study; T.T, K. Terui, and R.W. analyzed the mutations and status data; H.K., S. Ohga, A.O., S.K., T.K., K.G., K.K., T.M., and N.M. analyzed the status data; A.M., H.M., K. Takizawa, T.M., and K.Y., performed the research and analyzed the data; E.I. and I.H. designed the study and analyzed the data; and all authors wrote the manuscript.

Conflict-of-interest disclosure: The authors declare no competing financial interests.

Correspondence: Isao Hamaguchi, MD, PhD, Department of Safety Research on Blood and Biological Products, National Institute of Infectious Diseases, 4-7-1, Gakuen, Musashimurayama, Tokyo 208-0011, Japan; e-mail: 130hama@nih.go.jp; or Etsuro Ito, MD, PhD, Department of Pediatrics, Hirosaki University Graduate School of Medicine, 5 Zaifucho, Hirosaki, Aomori 036-8562, Japan; e-mail: eturou@cc.hirosaki-u.ac.jp.

References

1. Hamaguchi I, Flygare J, Nishiura H, et al. Proliferation deficiency of multipotent hematopoietic progenitors in ribosomal protein S19 (RPS19)-deficient diamond-Blackfan anemia improves following RPS19 gene transfer. *Mol Ther.* 2003;7(5 pt 1):613-622.
2. Vlachos A, Ball S, Dahl N, et al. Diagnosing and treating Diamond Blackfan anaemia: results of an international clinical consensus conference. *Br J Haematol.* 2008;142(6):859-876.
3. Draptchinskaia N, Gustavsson P, Andersson B, et al. The gene encoding ribosomal protein S19 is mutated in Diamond-Blackfan anaemia. *Nat Genet.* 1999;21(2):169-175.
4. Doherty L, Sheen MR, Vlachos A, et al. Ribosomal protein genes RPS10 and RPS26 are commonly mutated in Diamond-Blackfan anemia. *Am J Hum Genet.* 2010;86(2):222-228.
5. Gazda HT, Sheen MR, Vlachos A, et al. Ribosomal protein L5 and L11 mutations are associated with cleft palate and abnormal thumbs in Diamond-Blackfan anemia patients. *Am J Hum Genet.* 2008;83(6):769-780.
6. Farrar JE, Nater M, Caywood E, et al. Abnormalities of the large ribosomal subunit protein, Rpl35a, in Diamond-Blackfan anemia. *Blood.* 2008;112(5):1582-1592.
7. Gazda HT, Grabowska A, Merida-Long LB, et al. Ribosomal protein S24 gene is mutated in Diamond-Blackfan anemia. *Am J Hum Genet.* 2006; 79(6):1110-1118.
8. Konno Y, Toki T, Tandai S, et al. Mutations in the ribosomal protein genes in Japanese patients with Diamond-Blackfan anemia. *Haematologica.* 2010;95(8):1293-1299.
9. Robledo S, Idol RA, Crimmins DL, Ladenson JH, Mason PJ, Bessler M. The role of human ribosomal proteins in the maturation of rRNA and ribosome production. *RNA.* 2008;14(9):1918-1929.
10. Léger-Silvestre I, Caffrey JM, Dawaliby R, et al. Specific Role for Yeast Homologs of the Diamond Blackfan Anemia-associated Rps19 Protein in Ribosome Synthesis. *J Biol Chem.* 2005;280(46): 38177-38185.
11. Choesmel V, Fribourg S, Aguissa-Toure AH, et al. Mutation of ribosomal protein RPS24 in Diamond-Blackfan anemia results in a ribosome biogenesis disorder. *Hum Mol Genet.* 2008;17(9):1253-1263.
12. Flygare J, Aspesi A, Bailey JC, et al. Human RPS19, the gene mutated in Diamond-Blackfan anemia, encodes a ribosomal protein required for the maturation of 40S ribosomal subunits. *Blood.* 2007;109(3):980-986.
13. Quarello P, Garelli E, Brusco A, et al. Multiplex ligation-dependent probe amplification enhances molecular diagnosis of Diamond-Blackfan anemia due to RPS19 deficiency. *Haematologica.* 2008; 93(11):1748-1750.
14. Yamamoto G, Nannya Y, Kato M, et al. Highly sensitive method for genomewide detection of allelic composition in nonpaired, primary tumor specimens by use of affymetrix single-nucleotide-polymorphism genotyping microarrays. *Am J Hum Genet.* 2007;81(1):114-126.
15. Song MJ, Yoo EH, Lee KO, et al. A novel initiation codon mutation in the ribosomal protein S17 gene (RPS17) in a patient with Diamond-Blackfan anemia. *Pediatr Blood Cancer.* 2010;54(4):629-631.
16. Cmejla R, Cmejlova J, Handrkova H, Petrak J, Pospisilova D. Ribosomal protein S17 gene (RPS17) is mutated in Diamond-Blackfan anemia. *Hum Mutat.* 2007;28(12):1178-1182.
17. Cmejla R, Cmejlova J, Handrkova H, et al. Identification of mutations in the ribosomal protein L5 (RPL5) and ribosomal protein L11 (RPL11) genes in Czech patients with Diamond-Blackfan anemia. *Hum Mutat.* 2009;30(3):321-327.
18. Quarello P, Garelli E, Carando A, et al. Diamond-Blackfan anemia: genotype-phenotype correlations in Italian patients with RPL5 and RPL11 mutations. *Haematologica.* 2010;95(2):206-213.
19. Boria I, Garelli E, Gazda HT, et al. The ribosomal basis of Diamond-Blackfan Anemia: mutation and database update. *Hum Mutat.* 2010;31(12):1269-1279.
20. Campagnoli MF, Garelli E, Quarello P, et al. Molecular basis of Diamond-Blackfan anemia: new findings from the Italian registry and a review of the literature. *Haematologica.* 2004;89(4):480-489.
21. Willig TN, Draptchinskaia N, Dianzani I, et al. Mutations in ribosomal protein S19 gene and diamond blackfan anemia: wide variations in phenotypic expression. *Blood.* 1999;94(12):4294-4306.
22. Gustavsson P, Garelli E, Draptchinskaia N, et al. Identification of microdeletions spanning the Diamond-Blackfan anemia locus on 19q13 and evidence for genetic heterogeneity. *Am J Hum Genet.* 1998;63(5):1388-1395.

Frequent somatic mosaicism of *NEMO* in T cells of patients with X-linked anhidrotic ectodermal dysplasia with immunodeficiency

Tomoki Kawai,[1] Ryuta Nishikomori,[1] Kazushi Izawa,[1] Yuuki Murata,[1] Naoko Tanaka,[1] Hidemasa Sakai,[1] Megumu Saito,[2] Takahiro Yasumi,[1] Yuki Takaoka,[1] Tatsutoshi Nakahata,[2] Tomoyuki Mizukami,[3] Hiroyuki Nunoi,[3] Yuki Kiyohara,[4] Atsushi Yoden,[5] Takuji Murata,[5] Shinya Sasaki,[6] Etsuro Ito,[6] Hiroshi Akutagawa,[7] Toshinao Kawai,[8] Chihaya Imai,[9] Satoshi Okada,[10] Masao Kobayashi,[10] and Toshio Heike[1]

[1]Department of Pediatrics, Kyoto University Graduate School of Medicine, Kyoto, Japan; [2]Clinical Application Department, Center for iPS Cell Research and Application, Institute for Integrated Cell-Material Sciences, Kyoto University, Kyoto, Japan; [3]Division of Pediatrics, Department of Reproductive and Developmental Medicine, Faculty of Medicine, University of Miyazaki, Miyazaki, Japan; [4]Department of Pediatrics, Faculty of Medicine, Osaka University, Suita, Japan; [5]Department of Pediatrics, Osaka Medical College, Takatsuki, Japan; [6]Department of Pediatrics, Hirosaki University Graduate School of Medicine, Hirosaki, Japan; [7]Department of Pediatrics, Kishiwada City Hospital, Kishiwada, Japan; [8]Department of Human Genetics, National Center for Child Health and Development, Tokyo, Japan; [9]Department of Pediatrics, Niigata University, Niigata, Japan; and [10]Department of Pediatrics, Hiroshima University Graduate School of Biomedical Sciences, Hiroshima, Japan

Somatic mosaicism has been described in several primary immunodeficiency diseases and causes modified phenotypes in affected patients. X-linked anhidrotic ectodermal dysplasia with immunodeficiency (XL-EDA-ID) is caused by hypomorphic mutations in the *NF-κB essential modulator (NEMO)* gene and manifests clinically in various ways. We have previously reported a case of XL-EDA-ID with somatic mosaicism caused by a duplication mutation of the *NEMO* gene, but the frequency of somatic mosaicism of *NEMO* and its clinical impact on XL-EDA-ID is not fully understood. In this study, somatic mosaicism of *NEMO* was evaluated in XL-EDA-ID patients in Japan. Cells expressing wild-type NEMO, most of which were derived from the T-cell lineage, were detected in 9 of 10 XL-EDA-ID patients. These data indicate that the frequency of somatic mosaicism of *NEMO* is high in XL-ED-ID patients and that the presence of somatic mosaicism of *NEMO* could have an impact on the diagnosis and treatment of XL-ED-ID patients. (*Blood.* 2012;119(23):5458-5466)

Introduction

X-linked anhidrotic ectodermal dysplasia with immunodeficiency (XL-EDA-ID) is a disease with clinical features including hypohidrosis, delayed eruption of teeth, coarse hair, and immunodeficiency associated with frequent bacterial infections.[1-5] The gene responsible for XL-EDA-ID has been identified as *NF-κB essential modulator (NEMO)*.[6-8] NEMO is necessary for the function of IκB kinase, which phosphorylates and degrades IκB to activate NF-κB.[9-10] Defects in NEMO cause various abnormalities in signal transduction pathways involving NF-κB, and affect factors such as the IL-1 family protein receptors, the TLRs, VEGFR-3, receptor activator of nuclear factor κB (RANK), the ectodysplasin-A receptor, CD40, and the TNF receptor I.[7] Whereas a complete loss of NEMO function in humans is believed to cause embryonic lethality,[11] *NEMO* mutations in XL-EDA-ID patients are hypomorphic,[8] causing a partial loss of NEMO functions.

In XL-EDA-ID, NEMO defects lead to diverse immunologic features including susceptibility to pathogens, impaired Ab response to polysaccharides,[2,4,12] hypogammaglobulinemia,[13] hyper IgM syndrome,[14] and impaired NK-cell activity,[15] with a large degree of variability in phenotypes among the patients. For example, approximately one-tenth of XL-EDA-ID patients exhibit reduced mitogen-induced proliferation of T lymphocytes.[12] Moreover, one-fourth suffer from inflammatory disorders such as inflammatory bowel disease and rheumatoid arthritis,[12] although the inflammatory process usually relies on NF-κB activation.[16] One explanation for this clinical variability is that the XL-EDA-ID phenotype is *NEMO* genotype-specific. Although the XL-EDA-ID database reported by Hanson et al succeeds to some extent in linking the specific clinical features to *NEMO* genotype,[12] the penetrance of some clinical features is not high and the mechanism accounting for this variability is unknown.

Recently, we have reported a case of spontaneous reversion mosaicism of the *NEMO* gene in XL-EDA-ID, which showed an atypical phenotype involving decreased mitogen-induced T-cell proliferation along with decreased CD4 T cells (patient 1).[17] There have been no subsequent reports on somatic mosaicism in XL-EDA-ID, and its prevalence and impact on the clinical features of the disease is unknown. In this study, we describe the younger brother of patient 1, who suffered from XL-EDA-ID with the same mutation and somatic reversion mosaicism of *NEMO*. Patient 2 showed intriguing laboratory findings in that mitogen-induced T-cell proliferation varied in accordance with the rate of detected reversion in the peripheral blood. These 2 cases led us to perform a nationwide study of XL-EDA-ID patients in Japan that revealed a high incidence of somatic mosaicism of *NEMO*.

Submitted May 11, 2011; accepted April 8, 2012. Prepublished online as *Blood* First Edition paper, April 19, 2012; DOI 10.1182/blood-2011-05-354167.

The online version of this article contains a data supplement.

The publication costs of this article were defrayed in part by page charge payment. Therefore, and solely to indicate this fact, this article is hereby marked "advertisement" in accordance with 18 USC section 1734.

Table 1. Clinical and genetic features of XL-EDA-ID patients

Patient	Mutation	Ectodermal dysplasia	Mitogen-induced proliferation	Infections	Complications	Therapy	Sex chromosome chimerism
1	Duplication	+	Reduced	Sepsis (S.P. and P.A.)	Chronic diarrhea	IVIG	100% XY
				Disseminated M.A.C.	Failure to thrive	RFP, CAM, AMK, EB	
				Skin abscess (S.A.)	Small intestinal stenosis	Rifabutin	
				Invasive *Aspergillus*	Lymphedema		
2	Duplication	+	Reduced	Sepsis (*E coli*)	Failure to thrive	IVIG, ST, EB, CAM	99.8% XY 0.2% X
				Disseminated M.S.		Rifabutin, SCT	
3	D311E	−	Normal	Disseminated B.C.G.		IVIG, INH	100% XY
				Sepsis (S.P.)		RFP, SCT	
4	A169P	+	Normal	Meningitis (S.P.)	IBD	IVIG, ST, PSL	99% XY
					Interstitial pneumonia	CyA, MTX, Infliximab	
					Rheumatoid arthritis		
5	L227P	+	Normal	Recurrent pneumonia	IBD	ST, mesalazine	Not done
				Pyogenic coxitis		Infliximab	
				Recurrent otitis media			
6	R182P	+	Not done	Recurrent otitis media	IBD	ST, mesalazine	99.8% XY 0.2% X
				UTI, Recurrent stomatitis			
				Subepidermal abscess			
7	R175P	+	Normal	Recurrent sepsis (S.P.)		IVIG	100% XY
8	Q348X	+	Normal	Disseminated B.C.G.	IBD	IVIG, ST	100% XY
9	R175P	+	Normal	Recurrent pneumonia	IBD	IVIG	100% XY
				Recurrent otitis media		5-aminosalicylic acid	
				Kaposi varicelliform eruption			
10	1167 ins C	+	Normal	Sepsis and Enteritis (E.A)	Failure to thrive	IVIG, SCT	Not done
				Sepsis (C.G.)	Pyloric stenosis, colon polyps		
				UTI (K.P.)			

S.P. indicates *Streptococcus pneumoniae*; P.A., *Pseudomonas aeruginosa*; IVIG, intravascular immunoglobulin infusion; M.A.C., *Mycobacterium avium* complex; S.A., *Staphylococcus aureus*; *E coli*, *Escherichia coli*; ST, trimethoprim-sulfamethoxazole; M.S., *Mycobacterium szulgai*; AMK, amikacin; EB, ethambutol; CAM, clarithromycin; SCT, stem cell transplantation; B.C.G., Bacille de Calmette et Guerin; INH, isoniazid; RFP, rifampicin; IBD, inflammatory bowel disease; PSL, prednisolone; CyA, cyclosporine A; MTX, methotrexate; UTI, urinary tract infection; E.A., *Enterobacter aerogenes*; C.G., *Candida glabrata*; and K.P., *Klebsiella* pneumonia.

Methods

Informed consent

Informed consent was obtained from the patients and their families following the Declaration of Helsinki according to the protocol of the Internal Review Board of Kyoto University, which approved this study.

Patients

Patient 1 was an XL-EDA-ID patient with a duplication mutation of the *NEMO* gene spanning intron 3 to exon 6. This patient has been reported previously[17] and died from an *Aspergillus* infection at the age of 4. Patient 2, born at term, was the younger brother of patient 1. This patient was also diagnosed as XL-EDA-ID with the same duplication mutation as patient 1 by genetic study. He received trimethoprim-sulfamethoxazole prophylaxis and a monthly infusion of immunoglobulin from the age of 1 month. The patient maintained good health and had a body weight of 7899*g* at 6 months when he started to fail to thrive. Except for poor weight gain, patient 2 appeared active with a good appetite, negative C-reactive protein, normal white blood cell counts, and no apparent symptoms. At 19 months of age, *Mycobacterium szulgai* was detected by venous blood culture, and the patient was treated with multidrug regimens including ethambutol, rifabutin, and clarithromycin based on the treatment of systemic *Mycobacterium avium* complex infection. The patient responded well to the treatment and his weight increased from 7830*g* to 9165*g* within a month after the treatment was initiated. Patient 2 received an unrelated cord blood cell transplantation at 26 months of age, containing 8.5×10^7 nucleated cells/kg (4.4×10^5 $CD34^+$ cells/kg), which was matched at 5 of 8 loci: mismatches occurred at 1 HLA-B and 1 HLA-C allele (according to serology), and at 1 HLA-A, 1 HLA-B, and 1 HLA-C allele (according to DNA typing). The preconditioning regimen consisted of fludarabine (30 mg/m^2/d) on days −7 to −3, melphalan (70 mg/m^2/d) on days −6 to −5, and rabbit anti-thymocyte globulin (2.5 mg/kg/d) on days −6 to −2. At first, Tacrolimus (0.024 mg/kg/d) was used to prevent GVHD, but this was switched to cyclosporin A (3 mg/kg/d) on day 9 because of drug-induced encephalopathy. Neutrophil ($> 0.5 \times 10^9$/L) and platelet ($> 50 \times 10^9$/L) engraftment were examined on days 13 and 40, respectively. Although $CD19^+$ cells (2042/μL, 94% donor chimerism), $CD56^+$ cells (242/μL, 97% donor chimerism), and monocytes (557/μL, 69% donor chimerism) were successfully generated, $CD3^+$ cells were not detected in the peripheral blood by day 54. The patient suffered from septic shock and died on day 60. Patients 3 to 10 were XL-EDA-ID patients recruited nationwide in Japan. Clinical details of patients 3, 4, and 10 have been reported previously.[18-20] These patients had clinical phenotypes characteristic of XL-EDA-ID such as ectodermal dysplasia, innate and/or acquired immunity defects, and susceptibility to pyogenic bacteria and *Mycobacterium* infection. Every patient had a mutation in the *NEMO* gene that caused reduced NF-κB activation in a NEMO reconstitution assay, as described in "Proliferation of $NEMO^{normal}$ and $NEMO^{low}$ T cells." Patient profiles are listed in Table 1.

Flow cytometric analysis

NEMO intracellular staining was performed as previously described.[17] The cells were stained for the following lineage markers before staining for NEMO: CD4, CD8, CD14, CD15, CD19, CD56, CD45RA (BD Biosciences/BD Pharmingen), and CCR7 (R&D Systems Inc). Intracellular staining of human IFN-γ, TNF-α, and NEMO was performed as previously described.[18] The stained cells were collected using a FACSCalibur flow cytometer (BD Biosciences) and analyzed using the FlowJo software (TreeStar).

Reporter assay

Wild-type and mutant *NEMO* cDNAs were generated from a healthy volunteer and the recruited XL-EDA-ID patients by RT-PCR; the cDNAs were subcloned into the p3xFLAG-CMV14 vector (Sigma-Aldrich). NEMO null rat fibroblast cells (kindly provided by Dr S. Yamaoka, Department of Molecular Virology, Graduate School of Medicine, Tokyo Medical and Dental University, Tokyo, Japan) were plated at a density of

3×10^4 cells/well in a 24-well culture dish and were transfected with 40 ng of NF-κB reporter plasmid (pNF-κB-Luc; BD Biosciences/BD Clontech), 2 ng of *NEMO* mutant expression construct, 10 ng of internal control for the normalization of transfection efficiency (pRL-TK; Toyo Ink), and 148 ng of mock vector using FuGENE HD Transfection Reagent (TOYO-B-Net) according to the manufacturer's protocol. Twelve hours after transfection, the cells were stimulated with 15 ng/mL lipopolysaccharide (LPS; Sigma-Aldrich) for 4 hours and the NF-κB activity was measured using the PicaGene Dual SeaPansy assay kit (TOYO-B-Net). Experiments were performed in triplicate and firefly luciferase activity was normalized to *Renilla* luciferase activity.

Subcloning analysis of cDNA

Cell sorting of the various cell lineages was performed by FACSVantage (BD Biosciences). The purity of each lineage was > 95%. The cDNA from sorted cells was purified and reverse transcribed by Super Script III (Invitrogen) with random hexamers and amplified by the proofreading PCR enzyme KOD, as previously described.[17,21] The PCR primers used were NEMO2 (5′-AGAGACGAAGGAGCACAAAGCTGCCTTGAG-3′) and NEMO3 (5′-ACTGCAGGGACAATGGTGGGTGCATCTGTC-3′). The PCR products were subcloned using a TA cloning kit (Invitrogen) and sequenced by ABI 3130xl Genetic analyzer (Applied Biosystems). To determine whether additional mutations occurred in revertant subclones that had wild-type sequence in the original mutation site, the entire coding region of the *NEMO* gene was sequenced and an additional mutation was considered present when the same mutation was detected in multiple subclones.

Allele-specific PCR

The mRNA purified from sorted T cells and monocytes was reverse-transcribed by SuperScript III (Invitrogen) with the gene-specific primer NEMO2 and amplified by the proofreading PCR enzyme KOD (Toyobo) using the primers NEMO3 and NEMO 4 (5′-TGTGGACACGCAGTGAAACGTGGTCTGGAG-3′). The PCR products were used as templates for allele-specific PCRs with Ex Taq polymerase (Takara Bio). Mutant and wild-type *NEMO* DNA was generated from each NEMO expression plasmid, mixed at graded ratios, and used as controls. PCR conditions and primer sequences are listed in supplemental Table 1 (available on the *Blood* Web site; see the Supplemental Materials link at the top of the online article).

Proliferation of NEMO^{normal} and NEMO^{low} T cells

To obtain PHA-induced T-cell blasts, PBMCs were stimulated with PHA (1:100; Invitrogen) and cultured in RPMI 1640 supplemented with 5% FCS and recombinant human IL-2 (50 IU/mL; kindly provided by Takeda Pharmaceutical Company) at 37°C for 7 days. Subcloning analysis of the cDNA obtained from the T-cell blasts was performed as described in "Subcloning analysis of cDNA."

Results

Reversion mosaicism of NEMO occurred in siblings with similar immunologic phenotypes

We previously reported patient 1 with a duplication mutation of the *NEMO* gene spanning intron 3 to exon 6, who was diagnosed as XL-EDA-ID at 1 year of age after suffering from recurrent infections.[17] At first, genetic diagnosis of the patient was difficult because the expression of aberrant *NEMO* mRNA was masked by the expression of normal *NEMO* mRNA by the revertant cells. Flow cytometric analysis of intracellular NEMO expression revealed cells with normal (NEMO^{normal}) and reduced (NEMO^{low}) levels of NEMO expression, indicating the presence of reversion mosaicism of the *NEMO* gene, and further analysis revealed that the *NEMO* mutation was disease-causing. PCR across the mutated region and sequencing of the PCR products revealed a duplication extending from intron 3 to exon 6, which was confirmed by Southern blot analysis. Additional copy number analysis of the *NEMO* gene of patient 1 and his mother excluded the possibility of a complex chromosomal aberration such as multiple duplication of the *NEMO* gene (supplemental Figure 1). Furthermore, polymorphism analysis using variable number tandem repeats on NEMO^{normal} and NEMO^{low} cells from patient 1 revealed that these cells were derived from the same origin (supplemental Table 2), indicating that the *NEMO* gene mosaicism was less likely because of amalgamation. The genomic analysis of the NEMO^{normal} cells revealed a complete reversion of the *NEMO* gene with no additional mutations. The clinical phenotype of patient 1 was combined immunodeficiency with a reduced number of T cells and mitogen-induced proliferation (Tables 2-3). We previously determined that reduced NEMO expression in the mutant T cells caused impairment of T-cell development and mitogen-induced proliferation.

Patient 2, the younger brother of patient 1, was diagnosed as XL-EDA-ID with the same duplication mutation as his brother. Flow cytometric analysis of intracellular NEMO expression performed at diagnosis showed that most of his PBMCs had reduced NEMO expression (Figure 1A). At 2 months of age, when most of the T cells were NEMO^{low}, absolute counts of the patient's T cells and the mitogen-induced proliferation of the patient's PBMCs were comparable with those of the healthy controls (Figure 1A-B; Table 2). These findings indicated that the *NEMO* mutation had no effect on T-cell development and mitogen-induced proliferation during early infancy in patient 2.

NEMO^{normal} T cells gradually increased as patient 2 grew older, while the absolute count of NEMO^{low} T cells decreased (Figure 1A-B). Accordingly, normal full-length *NEMO* cDNA, which had been undetectable in cord blood, was detectable in the patient's peripheral blood at 12 months of age. However, while NEMO^{normal} T cells were increasing, mitogen-induced T-cell proliferation started to decrease (Table 3), and the patient started to show poor weight gain from 6 months of age. When patient 2 was 17 months old, a blood culture revealed an *M szulgai* bacteremia. At this time, the absolute count of NEMO^{normal} T cells peaked, and NEMO^{low} T cells were at a minimum. He began to gain weight after anti-*Mycobacterium* medication was initiated, although NEMO^{normal} T cells started to decrease and NEMO^{low} T cells began to increase (Figure 1B). When the patient was 23 months old, mitogen-induced T-cell proliferation was still low and a roughly equal number of NEMO^{low} and NEMO^{normal} T cells were detected (Table 3). Overall, as patient 2 grew older, NEMO^{normal} T cells increased as the total number of T cells and the mitogen-induced T-cell proliferation decreased, similar to what had occurred in patient 1 at a similar age.

Various analyses were performed to compare the immunologic phenotype of NEMO^{low} and NEMO^{normal} T cells in detail. Both NEMO^{normal} and NEMO^{low} CD4$^+$ T cells carried a diverse Vβ repertoire, but CD8$^+$ T cells had a skewed Vβ repertoire regardless of NEMO expression level (Figure 1C). Surface marker analysis revealed that most of the NEMO^{normal} T cells were CD45RA$^-$/CCR7$^-$ and most of the NEMO^{low} T cells were CD45RA$^+$/CCR7$^+$ (Figure 1D). The NEMO^{normal} T cells produced similar amounts of IFN-γ and TNF-α as healthy control cells, while the production of these cytokines were reduced in NEMO^{low} T cells (Figure 1E-F). Taken together, these data implied that the immunologic phenotype of T cells from patient 2 converged with that of patient 1 as patient 2 grew older.

Table 2. Surface marker analysis of peripheral mononuclear cells of patients 1 and 2

	Patient 1	Patient 2		Healthy controls
Age at analysis	2 y	2 mo	19 mo	
CD3	1503	2366	1014	2997 ± 1751
CD4	292	1583	374	1683 ± 874
CD8	1160	783	547	1114 ± 976
TCRαβ	1386	2295	439	2620 ± 1612
TCRγδ	109	74	574	343 ± 177
$CD4^+CD45RA$	58	1336	105	1471 ± 890
$CD4^+CD45RO$	263	307	266	497 ± 189
$CD8^+CD45RA$	1178	783	297	1083 ± 1078
$CD8^+CD45RO$	361	21	250	385 ± 442
$CD4^+CD25$	80	427	93	210 ± 99
CD19	1200	941	1543	1252 ± 1145
CD20	1189	931	1536	1125 ± 837
$CD19^+$Sm-IgG	7	18	17	54 ± 21
$CD19^+$Sm-IgA	15	4	14	18 ± 14
$CD19^+$Sm-IgM	1171	910	1505	1057 ± 881
$CD19^+$Sm-IgD	1171	906	1495	1052 ± 884
CD16	912	176	24	287 ± 200
CD56	908	176	24	306 ± 207

Surface markers expressed by XL-EDA-ID patients' PBMCs are shown as absolute counts per microliter of peripheral blood. Healthy control values are based on children aged 1 to 6 years and are shown as the mean ± SD.

Sm indicates the surface membrane.

High incidence of somatic mosaicism of the *NEMO* gene in XL-EDA-ID patients

It is worth noting that somatic reversion mosaicism of the *NEMO* gene occurred in both of the 2 XL-EDA-ID siblings carrying a duplication mutation. To determine whether a high frequency of reversion is a specific event for this type of *NEMO* duplication mutation[22-25] or if the reversion of the *NEMO* gene occurs commonly in XL-EDA-ID patients, we recruited an additional 8 XL-EDA-ID patients from throughout Japan (Table 1) and analyzed the presence of *NEMO* reversion. These patients had various combinations of clinical phenotypes characteristic of XL-EDA-ID such as ectodermal dysplasia, innate and acquired immunity defects, and susceptibility to pyogenic bacteria and *Mycobacterium* infections. Every patient had a mutation of the *NEMO* gene with reduced NF-κB activation potential, as evaluated in a NEMO reconstitution assay (Figure 2).

Among the 8 patients, only patient 3 had a large proportion of $NEMO^{low}$ cells by flow cytometric analysis. The majority of patient 3's PBMCs were $NEMO^{low}$, whereas 10% of the patient's $CD8^+$ cells were $NEMO^{normal}$ (Figure 3A). This patient was identified as carrying the D311E mutation. Because missense mutations of the *NEMO* gene often do not result in the reduced expression of NEMO protein, subcloning and sequencing analysis was performed on the *NEMO* cDNA isolated from the remaining patients, and 6 of the 7 patients had normal *NEMO* subclones (Table 3). Expansion of maternal cells after fetomaternal transfusion was ruled out in these patients by FISH analysis with X and Y probes (Table 1).

Additional genetic analysis of the entire coding region of the *NEMO* gene was performed on $NEMO^{normal}$ cells from patient 3 and on reverted subclones from the other patients, except for patient 10 who had already received stem cell transplantation. The *NEMO* gene in these samples had reverted to wild-type with no additional mutations (Figure 3B and data not shown). To specifically determine in which cell lineages the reversion occurred, subcloning and sequencing analysis of cDNA in various cell lineages was performed. This analysis revealed that all the revertant cells were of the T-cell lineage and that no reversion occurred in monocytes and very little occurred in B cells (Table 4). Allele-specific PCR confirmed that reversion occurred in T cells but not in monocytes (Figure 4).

Selective advantage of $NEMO^{normal}$ cells in XL-EDA-ID carriers

The high frequency of somatic mosaicism in T cells of XL-EDA-ID patients indicated a strong selective advantage of wild-type NEMO T cells over T cells carrying mutant NEMO. To confirm this hypothesis, *NEMO* cDNA analysis was performed on various cell lineages from the mothers of the patients who are heterozygous for *NEMO* mutation and thus have mosaicism

Table 3. Immunologic analysis of patients 1 and 2

	Patient 1	Patient 2 (treated with IVIG)	
Age at analysis, mo	9	9	20
Serum immunoglobulin levels, g/L (control)			
IgG	10.63 (4.51-10.46)	8.44 (4.51-10.46)	10.37 (7.15-9.07)
IgA	1.36 (0.14-0.64)	1.88 (0.14-0.64)	3.93 (0.22-1.44)
IgM	0.4 (0.33-1.00)	0.17 (0.33-1.00)	0.20 (0.34-1.28)
Age at analysis	2 y	2 mo	23 mo
T-cell proliferation, SI (control)	9.3 (206.9 ± 142.5)	55.3 (64.8 ± 8.1)	7.2 (89.4 ± 31.2)

Control values of serum immunoglobulin levels are based on children aged either 7 to 9 months or 1 to 2 years and are shown as the mean ± SD. The T-cell proliferation assay was performed as described previously[17] with at least three healthy adults as controls.

SI indicates stimulation index; and IVIG, 2.5 g of monthly IV immune globulin infusion.